This document was prepared in conjunction with work accomplished under Contract No. DE-AC09-96SR18500 with the U. S. Department of Energy.

DISCLAIMER

WSRC-TR-2006-00003, REV. 0
SRNL-RPP-2006-00002, REV. 0

THE DEVELOPMENT OF LASER ABLATION-INDUCTIVELY COUPLED PLASMA- ATOMIC EMISSION AND MASS SPECTROSCOPY FOR THE ANALYSIS OF HANFORD HIGH LEVEL WASTE: PHASE II (U)

ANALYTICAL DEVELOPMENT

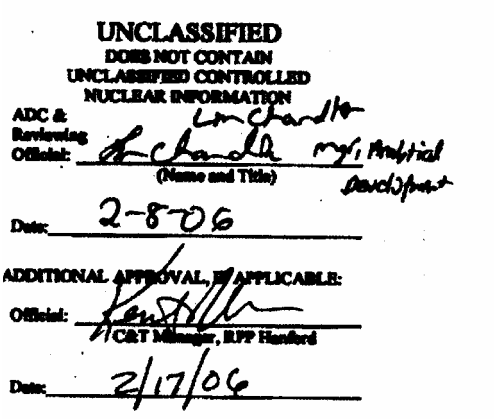

FEBRUARY 2006

Washington Savannah River Company
Savannah River Site
Aiken, SC 29808

Prepared for the U.S. Department of Energy Under Contract Number DEAC09-96SR18500

SRS savannah river site ™

DISCLAIMER

Printed in the United States of America

Prepared For
U.S. Department of Energy

WSRC-TR-2006-00003, REV. 0
SRNL-RPP-2006-00002, REV. 0

Key Words:
Laser ablation ICP-AES
Laser ablation ICP-MS
Radioactive glass, High level waste

Retention:
Permanent

Key WTP C&T References:
Statement of Work – CCN091850
Test Plan - WSRC-TR-2004-00447
Test Exception Plan – CCN130232

THE DEVELOPMENT OF LASER-ABLATION INDUCTIVELY COUPLED PLASMA ATOMIC EMISSION SPECTROSCOPY FOR THE ANALYSIS OF HANFORD HIGH LEVEL WASTE: PHASE II (U)

Kristine Eland Zeigler, SRNL
William T. Boyce, SRNL
Charles J. Coleman, SRNL
Damon R. Click, SRNL
Charles L. Crawford, SRNL

FEBRUARY 2006

Washington Savannah River Company
Savannah River Site
Aiken, SC 29808

Prepared for the U.S. Department of Energy Under Contract Number DE-AC09-96SR18500

SRS savannah river site ™

REVIEWS AND APPROVALS

Kristine Eland Zeigler — 2/8/06
K. E. Zeigler, Co-Author, Analytical Development, SRNL — Date

2/8/06
W. T. Boyce, Co-Author, Analytical Development, SRNL — Date

2/8/2006
C. J. Coleman, Co-Author, Analytical Development, SRNL — Date

Damon R Click — 2/8/06
D. R. Click, Co-Author, Analytical Development, SRNL — Date

C. L. Crawford — 2/8/06
C. L. Crawford, Co-Author, Advanced Process Development, SRNL — Date

L. L. Tovo — 2/8/06
L. L. Tovo, Technical Reviewer, Analytical Development, SRNL — Date

Connie C Herman — 2/8/06
C. C. Herman, RPP Program Manager, Process Engineering Technology, SRNL — Date

RE Edwards — 2/14/06
R. E. Edwards, Manager, RPP Project, Process Science & Engineering, SRNL — Date

Anna V. Arakali — 2/24/06
A. V. Arakali, C&T WTP Representative — Date

TABLE OF CONTENTS

LIST OF FIGURES

LIST OF TABLES

ABBREVIATIONS

AD	Analytical Development
ARG	Analytical Reference Glass
AY-102	AY-102/C106 glass sample
CPS	counts per second
GV	GV Isoprobe (ICP-MS; radioactive)
Hz	Hertz
HLW	High Level Waste
ICP-AES	Inductively Coupled Plasma Atomic Emission Spectroscopy
ICP-MS	Inductively Coupled Plasma Mass Spectrometry
JY	Jobin Yvon (170C ICP-AES; radioactive)
L/min	Liters per minute
LA	Laser Ablation
LA-ICP-AES	Laser Ablation Inductively Coupled Plasma Atomic Emission Spectroscopy
LA-ICP-MS	Laser Ablation Inductively Coupled Plasma Mass Spectrometry
μ	micron/microns
μ/s	microns per second
mJ	milliJoule
ms	milliseconds
MFPV	Melter Feed Preparation Vessel
MRQ	Minimum Reportable Quantity
nm	nanometer
ns	nanosecond
PE	Perkin Elmer (Optima 3000 ICP-AES ; non-radioactive)
PNWD	Pacific Northwest National Laboratory/Pacific Northwest Division
PQ2	Plasma Quad 2 (ICP-MS; radioactive)
psi	pounds per square inch
rf	radio frequency
S	AY-102/C106 simulant (unknown)
SCF	Shielded Cell Facility
SOW	Statement of Work
SRNL	Savannah River National Laboratory
TT&QA	Task Technical and Quality Assurance Plan
W	Watts
WTP	Hanford Tank Waste Treatment and Immobilization Plant

This page intentionally left blank.

1.0 EXECUTIVE SUMMARY

The task of developing analytical methods that provide rapid turnaround time, while providing sufficient accuracy and precision to determine waste and melter feed composition variations for the high level waste (HLW) vitrification process, was the work scope provided by Hanford Tank Waste Treatment and Immobilization Plant (WTP).[1-2] The specific approach for Phase II of the task was to use laser ablation-inductively coupled plasma-atomic emission spectroscopy (LA-ICP-AES) to determine the elemental composition of radioactive HLW sludge. This composition is representative of what is found in the Melter Feed Preparation Vessel (MFPV). It was shown in Phase I that LA-ICP-AES could provide fast analytical results on the composition of the MFPV after conversion to a glass puck. This method does not use any chemical dissolution and generates less waste then the typical wet chemistry dissolution methods. Although some of the specific criteria of the task plan could not be met in Phase I, such as the minimum reportable quantity for some elements, and greater than 10% precision and accuracy for some of the minor elements, the second phase of the work proceeded due to the recognition of the potential benefit of this technique. It was recommended in Phase I that several elements of interest outlined in the Work Scope be reviewed for process control necessity and interest since the target minimum reportable quantities (MRQ) were not all achievable.

The Phase II task was to demonstrate the optimized technologies from Phase I on radioactive material in a remote environment. The methodologies developed during these two phases would ultimately be implemented for production in the WTP analytical laboratory.[1] Although the task plan for Phase II specifically stated LA-ICP-AES work would be performed, due to extenuating circumstances, laser ablation of the radioactive sample could only be analyzed using LA-ICP-mass spectrometry (MS) after seeking WTP approval for test exception.[3] Despite the change from using MS instead of AES, these tasks are essential to proving the laser ablation method works to meet the criteria set forth by the Statement of Work and Task Plan.[1-2] The use of LA-ICP will aid in meeting the design production rates of the facility and ensuring that acceptable glass is produced.[1] This report summarizes data collected from Phase II work, from glass standards specifically created for this project encompassing the concentration range of AY-102,[a] and a path forward for continuation of LA-ICP-AES and –MS studies.

[a] SRNL has previously received and characterized a Hanford Tank 241- AY-102/C-106 sample.[4] After characterization, this High-Level Waste slurry was processed and vitrified into the ‘AY-102’ radioactive glass sample that was studied by the LA-ICP methods discussed in this report.

Results from Phase II work and the standards work include the following:

- Flat and smooth sample surfaces are extremely important for reproducible results.
- ICP-MS works very well for determining small concentrations within the glass; however concentrations over 5% saturated the detector.
- Use of the standards which encompassed the AY-102 concentration range did improve accuracy.
- Due to time constraints, operation parameters for ICP-MS could not be optimized fully. It will be essential that further optimization consistent with specific instruments and configuration will be required for the WTP Analytical Facility.
- Based on method performance and data collection, the less than 9 hour turn around time for analysis and data reporting still appear to be practical and feasible. Specific analysis time for standards and samples are dependent on the mode of analysis (ICP-AES or –MS).
- Abundance ratios of the radioactive isotopes of the AY-102/C106 glass agreed well with other non-LA isotopic ratio data from ICP-MS (specifically the uranium 234, 235, 236 and 238 isotopes).

The results obtained from analysis of the radioactive AY-102 glass using LA-ICP-MS was satisfactory and the task implementation was successful in demonstrating the laser ablation technique on the radioactive glass sample. The LA-ICP-MS AY-102 sample data compared well with previous data measured by ICP-AES and ICP-MS using chemical dissolution. Results from Phases I and II indicate that using LA-ICP-AES for analysis of the MFPV is feasible. LA-ICP-MS would work extremely well for low concentrations of analytes as well as for the radionuclides.

As stated in the recommendations for Phase I, and as well as that for Phase II, as the waste compliance strategy continues to be defined, it is highly recommended that WTP establishes achievable detection limits and associated uncertainties for the list of needed analytes for process monitoring and waste form compliance. Then, the developed method can truly be adapted and validated for WTP vitrification support. The data from Phase I and II work has proven that reliable results can be produced using LA-ICP-AES and –MS for a Hanford tank waste matrix.

2.0 INTRODUCTION

The WTP will prepare and process Hanford HLW streams into glass waste that meet requirements for HLW disposal. To begin the process, the HLW streams are transferred to the melter facility from the Pretreatment Facility and are received in the MFPV. In this tank, the HLW stream is blended with glass forming chemicals to produce an acceptable melter feed. Variations in the sludge retrieval, pretreatment, and vitrification processes will cause deviations in the nominal melter feed compositions and glass chemistry. It is necessary to have accurate, reproducible data for the ultimate disposition of the waste.

The Savannah River National Laboratory (SRNL) was requested by WTP via Statement of Work CCN091850[2] to develop laser ablation technology coupled with ICP-AES as a rapid analytical method for the analysis of feed samples from the MFPV. The target MRQ values for the elements of interest with a minimum requirement of sensitivity at least three times the method detection limit (i.e., 3x MDL) were defined in the Statement of Work[2] and the associated TT&QA Plan.[1] Target precision is <10% relative standard deviation. A Task Technical and Quality Assurance (TT&QA) Plan[1] was written to address Phase I and Phase II activities in support of developing the approach. This report documents data collected from Phase II activities. The results from Phase I were summarized in an earlier report.[5] The comparison of simulant data to that of radioactive AY-102 LA-ICP-AES data was not possible due to data collection on ICP-MS system for ablated radioactive AY-102 glass sample. An exception to the test plan, CCN130232,[3] was issued for changing the analysis technique to ICP-MS, due to the unavailability of the ICP-AES for radioactive analysis. Since the MFPV contains HLW both before and after addition of glass forming chemicals, elemental analysis methods are required for both types of samples (sludge only and sludge + glass forming chemicals).

The overall objective of this WTP task is to develop a LA-ICP-AES method to provide the rapid turnaround time (<9 hours) requested by the WTP, while providing sufficient accuracy and precision to determine waste and melter feed composition variations. The technique must be robust to compositional variations in order to meet the design production rates and to ensure that acceptable glass is produced. To complete the overall objective, the goal of the Phase II activities was to demonstrate the optimized technology from Phase I on radioactive material in a remote environment. Due to time constraints and instrument problems, the demonstration of the laser ablation technique was performed on the ICP-MS instead of the AES per WTP approved test exception.[3] Phase I analyses showed that the LA technique using ICP-AES was feasible with Hanford tank waste matrix simulant. The objective of the Phase II work was to show that these same results could be achieved on a radioactive sample. With the radioactive demonstration being performed using the ICP-MS, this further proved that the LA technique will work for both ICP-AES and –MS, in specific, for the analysis of MFPV.

Also included in this report are results from a set of five non-radioactive glasses, formulated to serve as calibration standards. The glasses were developed to encompass the concentration range of the AY-102 waste. The samples were prepared and developed[6] by the Process Science and Engineering Section and evaluated[7] by Statistical Consulting. These 5 glass standards contain all of the elements requested for analysis in the statement of work and the task plan (except Th and U), as well as an internal standard, scandium. These glasses were used to evaluate the need for a set of standard glasses that could be used in the WTP during ablation and analysis of glass disks prepared from various Hanford waste streams.

Overall, the implementation for task activities demonstrated the use of two different laser ablation units with widely accepted ICP analytical techniques (-AES, -MS) for Hanford tank waste matrix. The unique approach for this task was the use of applicable glass calibration standards that were prepared for bracketing the sample concentration range. Data generated from ablation of radioactive glass in an atypical setting was a success. However, the results have limited applicability to WTP because of different experimental configuration.

The steps taken for reconfiguring the LA and ICP systems for analyzing radioactive glass samples is described in Section 4.2. Data is discussed in Section 5.0 and 6.0 along with data taken from LA-ICP-AES on non-radioactive standards. Recommendations for further refinement are provided in Section 10.0. Data from Phase II are documented in two notebooks: WSRC-NB-2005-00036 and WSRC-NB-2005-00149. Applicable information is contained in this report along with experimental results.

3.0 MODIFICATIONS FOR RADIOACTIVE WORK

3.1 OVERVIEW

For Phase II of this project, due to the high radioactivity of the actual AY-102 sample, work had to be performed in a radioactive controlled environment. Since work was being performed in a radiochemical fume hood, specific limitations to the amount of radiation the worker was exposed to, as well as hood limits set for worker exposure control, needed to be considered. These issues included extremity (contact) dosage, whole body dosage determined ~30 centimeters from the radioactive source, and alpha contamination hood limits. Based on dose measurements from various radioactive Hanford samples and the actual AY-102 radioactive glass samples taken out of the SRNL Shielded Cell Facility (SCF) for other projects and experiments, it was calculated that 0.5 grams of AY-102 radioactive glass, shielded, could be removed from the SCF. This glass could then be transferred to a radiochemical fume hood for LA-ICP studies with appropriate shielding and distance from the worker. The radiation dose associated with the AY-102 glass sample was primarily from Sr-90/Y-90 beta emissions creating higher extremity doses relative to the penetrating Cs-137/Ba-137 whole body gamma dose.[4] The layout for experimental work required placing the laser unit in a radiochemical fume hood and interfacing with RadCon personnel for planning the activity within the established radiological control limits.

3.1.1 Hood

The particular radiochemical fume hood that was to be used to house the LA unit also contained the Analytical Development's (AD) GV Instruments Isoprobe-N ICP-MS. The reason the unit was placed in this hood and not the same hood as the JY 170C ICP-AES to be used for Phase II work was due to space constraints. Once the unit was placed inside the fume hood, it could no longer be used in a clean environment. Therefore, all of the electronics and power supplies were located on a cart just outside of the hood and the power cables were labeled as radioactive and once finished will also have to be declared radioactive waste. (The only power supply that is located in the fume hood is that of the LA control because the connections were not long enough to stretch outside of the fume hood.) The LA unit was placed on a dolly so that when it was not being used, it could be easily pushed back out of the way and when needed, brought near the front again. This dolly was also used to raise the unit off of the floor of the radiological fume hood so as not to disturb the air flow within.

3.1.2 Transfer Line

Another issue with the LA unit being in a different radiological fume hood than the ICP-AES torch was the transfer of the ablated particles. In this case, the LA unit and ICP-AES were in fume hoods directly across the room from each other. A stainless steel transfer line was built so that it exited one side of the fume hood, traveled up the side, across the top of the room and back down the opposite fume hood into the workspace.

Because this 30-foot transfer line was built of stainless steel, it was able to support its own weight. However, a bracket was attached and connected to a permanent fixture hanging from the ceiling of the room. Within the stainless steel tubing, ½ inch OD Tygon tubing was threaded through from one side to the other. This proved to be somewhat difficult as the stainless steel was already assembled before the tubing was threaded through it. A feed of stiffer tubing had to be threaded through the stainless steel to attach to the Tygon tubing to pull it back through to the other side. One issue with having this set-up is that the openings of the steel tubing were inside of the hood and anything used to guide the Tygon tubing through the stainless steel was considered contaminated and could not be reused.

It was determined that the stainless steel line was not needed for shielding because such a small amount of material was being transferred from the ablation chamber to the ICP torch. Even if all of the material became clogged in the Tygon tubing at one point, there still would not have been a radiation issue. The stainless steel line was merely used as a secondary container to hold the Tygon tubing up and out of the way.

3.1.3 Sample Holder

A special sample holder needed to be designed to shield the radioactive AY-102 (hot) sample as it was transported from the shielded cells where the glass was made to the radiological fume hood where it was to be analyzed. Calculations revealed that at a distance of 6 inches, using ¼ inch tungsten shielding, the amount of radiation from a 0.5 gram sample would be 106 milliRem per hour (mRem/hr), extremity (contact) dose. In hind sight, given that the data used to make these shielding calculations was high in Cs-137 content versus what the feed is now, this shielding was excessive. Calculations were performed by AD personnel using the Microshield Version 6.0 program from Groves Engineering.

The new shielded sample holder design used a ¼ inch tungsten chamber for shielding. This tungsten chamber was incorporated into the original square plastic holder design. A slide back top was constructed so that ¼ inch tungsten would help shield the top of the sample as well. As the sample holder was aligned to load into the sample chamber, the lid would slide back as the holder was being pushed into the chamber. This slide back top was constructed so the operator would never be directly exposed to the sample. The holder was aligned and loaded using a 6 inch removable handle, which was removed from the holder after finishing loading the chamber, and the chamber door closed. This 6 inch handle was designed to reduce the extremity exposure to the handler. When the analysis was finished, the handle was reattached to the holder, and the lid could slide back over the handle as the holder was pulled from the chamber. To ensure the lid would not slide off the top of the sample holder during transfer, a knob could be used to lock the top into place. Unfortunately, this knob was difficult to use in the shielded cells, so a cut piece of Styrofoam was used to hold the top and bottom together during transport. Within the tungsten chamber, a piece of adhesive was placed so that the glass could be pressed down and held in place when the holder was bagged and transferred out of the shielded cells.

3.1.4 Argon Flow Controller

Originally it was thought that the Ar gas needed to transfer the ablated sample to the ICP-AES could be taken from the GV ICP-MS, which sat next to the ablation unit. It would be a simple tee into the ICP-MS nebulizer gas line so that the flow of the argon could easily be software controlled by the ICP-MS software. Unfortunately there were problems encountered with this set-up. To use the nebulizer gas from the ICP-AES (across the room) would also pose a problem because a Tygon tubing line would be going in and out of a radioactive environment and also there was no room in the stainless steel line for 2 Tygon tubes.

Instead, the house argon was used. A pressure valve was placed in line and set to a pressure of 60 pounds per square inch (psi). This 60 psi line was fed into a MKS model 1179, 2000 standard cubic centimeters per minute (sccm) Mass Flow Controller with an MKS model 247D power supply and controller. The flow could be easily changed from 0.001 to 2 liters per minute (L/min) whenever needed. This flow line was then attached to the inlet of the LA unit. For this gas line setup, only the Tygon tubing line is entering the radiochemical fume hood with the mass flow controllers and valve remaining outside the fume hood.

3.1.5 Hardware

3.1.5.1 Laser Ablation Unit

The laser ablation unit that was used in the Phase II studies was a New Wave Research LUV 266 Merchentek EO. The main reason this unit was chosen to perform the radioactive work, as opposed to the Cetac LSX-100 unit used in Phase I work, was radiochemical fume hood space constraints. This system is an earlier version of the New Wave LA unit platforms, using a wavelength of 266 nanometer (nm) for ablation with spot sizes ranging from 5 to 400 microns (μ). Energy readings from the laser output were given in units of milliJoules (mJ) and mJ per second (mJ/sec) and were typically 1-4 mJ on the sample surface. The maximum repetition rate was 20 Hertz (Hz) and was user controlled. Software allowed the user to define set patterns of rastering, scanning or drilling. Because this unit was once to be used in a radioactive environment, it had been modified with steel casing around the bottom of the unit where the ablation chamber was located. This added one more layer of protection to the radioactive sample being analyzed.

3.1.5.2 ICP-AES for Elemental Analysis of Radioactive Glass

A Jobin-Yvon 170C ICP-AES radial instrument was to be used for elemental analysis before it encountered problems. The primary detection scheme is a Paschen-Runge spectrometer with 0.50 meter focal length. Photomultiplier tubes are located on the grating focal plane at wavelength positions of common elements. A 1.0 meter scanning monochromator is also available to select alternate lines from those fixed in the polychromator or to detect additional elements. A simple glass connector was used to connect the Tygon tubing carrying the ablated material to the bottom of the torch assembly.

3.1.5.3 ICP-MS for Elemental and Isotopic Analysis of Radioactive Glass

A GV Instruments IsoProbe-N multi-collector, magnetic sector ICP-MS was used for the radioactive LA demonstration. The collector section of the instrument houses 9 adjustable faraday cups, 7 Channeltron electron multipliers and one Daly detector. Only the faraday cups were used in this demonstration. For most of the measurements a single faraday cup was used. For Ba, Cs, and La isotopes, 7 of the 9 faradays were aligned and used to collect the responses of 7 different isotopes simultaneously.

The plasma torch box is mounted on a computer controlled motorized translation stage located in a radiological fume hood. The fume hood is specially designed to handle radioactive materials.

The normal liquid aspiration sample delivery system was used to set up the instrument. Instrument settings were optimized for response of the isotope/mass number of interest. Mass number identification was confirmed using High Purity, Inc., single element standards (10 part-per-million (ppm) as purchased diluted to 100 parts-per-billion (ppb) for a 1+ volt (V) faraday cup response. Typical detection limits for liquid samples are parts-per-trillion.

To perform the laser ablation determinations, after normal setup, the torch was shut down and the usual Cinnabar cyclonic spray chamber and 0.1 mL/min Glass Expansion nebulizer were detached from the standard plasma torch. The aerosol feed from the laser ablation unit was directly attached to the torch. Normal argon gas flow for the cool gas was used to ignite and run the instrument. The normal ICP nebulizer gas flow was replaced by an external argon source at a flow rate of about 1.5 L/min through the ablation chamber into the torch. Typical operating parameters for ICP-MS analyses include a cool gas flow rate of 14 L/min, intermediate gas flow of 1 L/min, nebulizer gas flow of 1 L/min, a radio frequency (rf) power of 1350 watts (W) and integration time of 1000 ms.

The full potential of the instrument and its operating software were not explored in this demonstration. Manual techniques were developed to locate the isotopes of interest, confirm the identity of those isotopes, and measure the Faraday Cup responses for those isotopes of interest.

3.1.5.4 Instrumentation Used In Phase I Work

For some radioactive LA data comparisons, Phase I data was used. The instruments used for Phase I data collection were a Cetac LA system and a Perkin Elmer Optima 3000 ICP-AES. These were the instruments also used in the testing of the standards. The Cetac LSX-200 Laser Ablation System had a wavelength output of 266 nm with ablation spot sizes ranging from 10 to 300 μ. Energy readings were displayed but these readings equate to the amount of light hitting a meter and were not an accurate measurement of the true energy of the pulse.

According to the laser manufacturer, the maximum output at 266 nm for a pulsewidth of 5 nanosecond (ns) is 15 mJ. However, the true energy at the sample surface is probably around 5 mJ. The repetition rate could be varied from 1- 20 Hz. The software allowed the user to program set patterns to run during ablation. These patterns included rastering, scanning a line, and drilling holes. The Perkin-Elmer Optima 3000 ICP-AES (PE ICP-AES) radial instrument was used for elemental analysis. The detector was a segmented-array charge coupled device allowing simultaneous multi-element measurements of line intensities and adjacent background.

Typical ICP-AES conditions, resulting from optimization studies included an rf power of 1400 W, a nebulizer gas flow rate of 0.65 L/min, an auxiliary gas flow rate of 0.5 L/min and a plasma gas flow rate of 15 L/min. At 200 nm, the resolution is 0.007 nm. Emission lines to monitor were chosen from the software according to their response and lack of interference. User friendly software allowed the collected data to be viewed in either number or graph form of intensity versus wavelength. More information on Phase I instruments and data can be found in Reference 5.

Also used for comparison was radioactive AY-102 data from previous RPP work.[8] In that previous work, dissolved samples of the AY-102 glass were submitted for analysis after mixed-acid dissolution of ground AY-102 glass powders that were <200 mesh size. Data in section 7.0 compares the use of the New Wave LA unit connected to the GV ICP-MS to the previous dissolution data[8] obtained from the JY 170C ICP-AES, as well as a VG Elemental Plasma Quad 2 ICP-MS. Appendix A presents data from the previous AY-102 glass dissolution study that compares various analyzed elemental results from the VG Elemental Plasma Quad 2 ICP-MS and the JY 170C ICP-AES.

4.0 STARTUP AND TROUBLESHOOTING

4.1 LA-ICP-AES

Initially, an extra 10 feet of tubing was left on the 25 feet of Tygon sample tubing which connected the LA unit outlet to the ICP-AES torch. Thus if there was tubing contamination, there would be no need to have to feed more tubing back through the stainless steel transfer line.

Upon startup, it was determined that no sample was being transferred through to the ICP-AES. This was extremely puzzling as the conditions had been mocked up on the cold ICP-AES system, using the same New Wave LA unit, before it was placed in the hood with its new sample holder. To quickly determine if sample was being transferred, a sample high in sodium content was ablated, as this will turn the plasma a bright orange color. Upon ablation, this did not occur, so it was thought that the problem may have been with the mass flow controller. The flow controller was a new aspect to the set-up since the ICP was not being used to control the nebulizer gas, nor was it coming through the ICP.

To identify if the flow controller was the problem, it was taken to the clean Cetac LA unit and PE ICP-AES for mock-up. Because of the way the gas lines are set up for the cold ICP-AES system, the flow controller was placed closer to the inlet of the LA unit as opposed to how it was for the radioactive setup, about 30 feet away from the inlet of the LA unit. Although it seemed that not much flow was occurring through the tubing, signal was still obtained on the cold ICP-AES and the flame turned bright orange with the sodium glass sample.

In the radioactive setup, the pressure of the gas was increased from 40 psi to 60 psi and the actual flow was increased from less than 1 L/min to 1.5 to 2 L/min. The controller was placed back in the radioactive setup as it had been placed in the cold mock-up, as well as the extra transfer tubing being trimmed to eliminate any extra length from the gas lines going to and from the ablation unit and the ICP torch. Again, upon ablation of the sodium glass, the plasma did not turn orange.

The next potential problem/difference considered was the 45-50° angle of the stainless steel transfer line through which the Tygon tubing was threaded. The angle may have been too steep an initial climb for the particles to flow. Calculations were performed to check if the particles were falling out of the argon gas mixture due to the climb. According to these calculations, particle suspension should have been possible.

Therefore, the transfer line from the LA unit to the torch was mocked up on the cold ICP-AES system with a sharp incline as it came out of the unit and with a sharp angle in to the ICP torch. Again, ablation particles were being transferred easily with the same conditions used for the New Wave LA unit.

Another potential problem identified was insufficient material being ablated such that no signal was seen. The settings on the New Wave LA unit for radioactive work were 100% power, around 2 mJ, with a spot size of 250 μ (largest possible is 400 μ). Although the exact power of the cold testing Cetac LA unit is unknown, it is probably around 5 mJ. Therefore, the power was lowered on the Cetac unit to mimic the New Wave unit. At this point, no signal was seen and the behavior on the sample surface during ablation mimicked the behavior that was being seen when using the New Wave unit in the radioactive environment. During this time, the JY ICP-AES began to have troubles with referencing and data collection. (Subsequent troubleshooting and vendor maintenance has revealed that the JY ICP-AES problem lay with a motorized filter.) It is unknown at this point whether the problem with the data collection was with the New Wave LA unit or the JY ICP-AES.

4.2 LA-ICP-MS

Fortunately, another option available for troubleshooting problems was the availability of the GV ICP-MS unit in the same hood as the LA unit. A short transfer line was connected from the LA unit to the ICP-MS torch to determine if the MS measured any signal. Signal was observed. The transfer line was then lengthened and mocked up at steep angles (to the best it could be done in the available space) as to mimic the lines traveling out and over to the ICP-AES. Again signal was measured. To further prove the LA set-up was not the problem, the Tygon sample tubing through the stainless steel transfer line was connected from the New Wave LA unit to the other JY ICP-AES end. In the JY ICP-AES hood, the sample tubing was connected to another piece of Tygon tubing that stretched straight back across the room to the ICP-MS torch. A sample of AZ-101 containing 0.07% lead oxide (PbO_2) was ablated and the signal measured by the GV ICP-MS is shown in Figure 1. The three different peaks shown in Figure 1 are attributed to the three naturally occurring isotopes of lead (Pb-206 at 24% abundance, Pb-207 at 22% abundance and Pb-208 at 52% abundance). The decreasing Pb lines within each of the three mass peaks represent the decay of the signal after the laser is turned off. This figure also shows the excellent sensitivity of the ICP-MS, especially when over 50 feet of tubing was used to carry the ablated material to the torch.

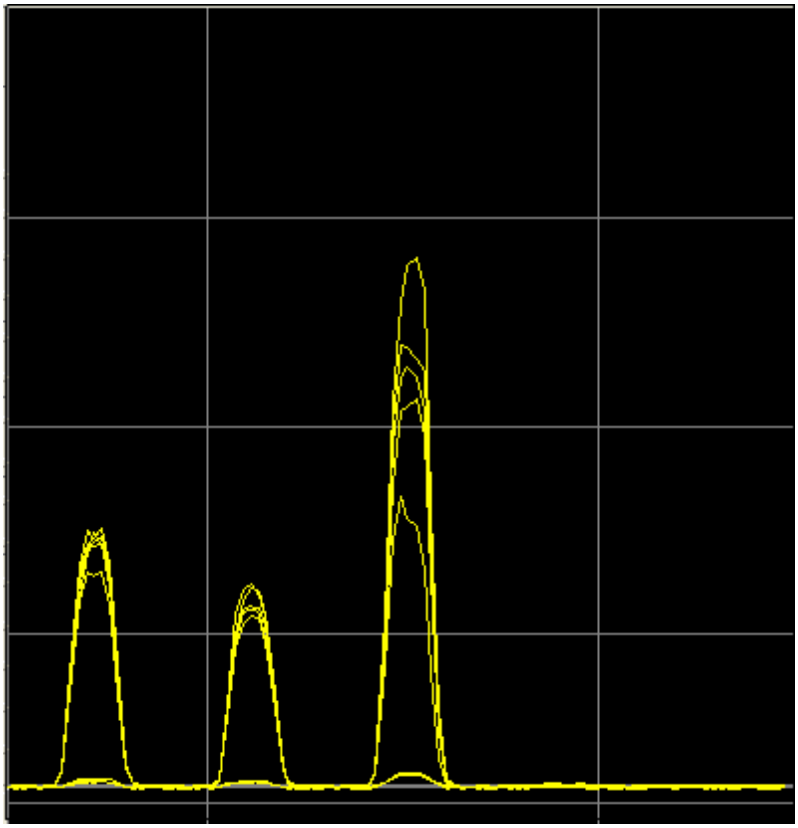

Figure 1. LA-ICP-MS signal of 0.07 wt% oxide of Pb 206, 207, and 208

At this point in time, the JY ICP-AES was completely out of service. There was not another opportunity to try and ablate sample and collect it with the ICP-AES after all of the troubleshooting was performed. For now, there is no definitive answer why signal was not seen using the New Wave LA unit and JY ICP-AES.

Due to a contamination event and sub-contracting issues, it would be some time before the JY vendor could return for troubleshooting and the ICP-AES be restored to operating conditions. A request was submitted to WTP for a test exception that would not change the work scope or objective but will allow the use of ICP-MS for task completion. Another reason for this request was the AY-102 glass was scheduled to be packaged and returned to Hanford the first week in December. Unfortunately, this date was not flexible so all work involving the AY-102 glass had to be finished by that first week. The test exception[3] was approved for LA-ICP-MS to begin.

4.2.1 LA Parameters

Due to the time constraints, optimization studies were not performed. The laser parameters, found in Table 1, were those used for LA-ICP-MS studies. Due to the sensitivity of the ICP-MS, it was difficult to use the same laser parameters for all the elements analyzed because of signal saturation of the detector. Decreasing the power in the cases of the Mn, Zn and Sb was not enough and the actual spot size had to be decreased as well. Unfortunately, as will be seen, the deviations for the element Mn are large because of the very low power used, which caused fluctuations in the power. This low power was needed to obtain signal without saturating the detector.

Table 1. New Wave LA conditions used for data collection with ICP-MS

Element	Spot size	Power	Neb Flow
Cr	250 μ	100% (2-4mJ)	1.5 L/min
Mn	100 μ	20% (~0.03mJ)	1.5 L/min
Zn	100 μ	40% (~0.40mJ)	1.5 L/min
Sb	100 μ	50% (~0.50mJ)	1.5 L/min
U	250 μ	100%	1.5 L/min
Pb	250 μ	100%	1.5 L/min
Ba	250 μ	100%	1.5 L/min
Th	250 μ	100%	1.5 L/min
Sc	250 μ	50%	1.5 L/min
Zn	100 μ	80% (~1.4mJ)	1.5 L/min

The nebulizer flow was increased from the Phase I work due to what was thought to be Ar flow problems before the study began. This flow rate of 1.5 L/min gave decent results without extinguishing the plasma. During sample change out, the flow rate had to be decreased or the system bypassed so that the plasma would not extinguish. On several occasions, the plasma had to be re-lit due to this extinguishing problem.

Another issue during data collection was surface availability for sampling. This was especially a problem for the radioactive AY-102 sample because it was a small sample to begin with and the surface was not flat. During some of the data collection, the raster pattern was programmed to repeat over the same sample area so that the ICP-MS would have enough time to collect the signal. This did reflect in the signal counts as they would increase slightly as the pattern was retraced. During this retracing, one could also increase the focal depth. The 2 glass samples that had this problem of uneven sample surface were the radioactive AY-102 spiked with 4.47% scandium oxide and an Analytical Reference Glass[9] (ARG) sample spiked with 4.62% scandium oxide, both of which were mounted in the shielded cells by remote handling. This sampling issue does reflect in the high deviations of the calculations. Although optimization studies were not performed for LA-ICP-MS during this phase, because neither of the actual systems for these tests performed here at SRNL will be used in the WTP Analytical Facility, optimization studies will have to be performed on the actual installed system.

4.2.2 ICP-MS Conditions

Due to the way that this ICP-MS system is set-up, only a small mass range can be analyzed. One must set the system to monitor the mass peak of interest, record the background, pre-ablate the sample until steady state is reached (around 1-2 minutes), and then collect the data. Once that element is finished, the MS must be moved to the next mass range of interest and the same steps followed. Although programs within the software can be set-up that will monitor the specific mass, one still must monitor the peak because the cups tend to move slightly as the instrument continues to warm over time.

Table 2 shows the data collection conditions of integration time and accumulations used. The number of accumulations used depended on the amount of time available for analysis.

Table 2. Conditions used for data collection with the ICP-MS

	Mass or Range	Integration time	Accumulations	Replicates
Cr	52	1000 ms	12	5
Mn	55	1000 ms	60	5
Sb	121	1000 ms	60	5
Zn	66	1000 ms	60	5
Pb	208	1000 ms	12	5
Actinides	233-242	1000 ms	12	5
Ba isotopes	134-138	5000 ms	12	5

5.0 DATA ANALYSIS

Within the GV ICP-MS IsoLynx software, a mean, standard deviation, standard error and the number of accumulations taken and included in the mean are provided in a data output file. An example of typical outputs from standards and the AY-102 sample can be seen in Table 3. The program determined whether a measurement was included in the final average (after) using a 2σ evaluation. These calculations are seen as the mean (after), standard deviation % (after) and error % (after). The number of measurements included in the mean and the total number collected are then shown. Next, the mean (before) is shown which includes all of the data collected before the 2σ evaluation, followed by the standard deviation, standard deviation % and standard error % for all the measurements in that replicate. In this example, all of the data is in units of counts per second (CPS).

Table 3. Typical ICP-MS data readout

Name	Mean (After)	Std Dev% (After)	Std Err% (After)	Incld	Total	Mean (Before)	Std Dev	Std Dev%	Std Err%
Cr52	7.6179E+07	4.856	1.464	11	12	7.5301E+07	4.655E+06	6.181	1.784
Zn66	5.7062E+07	11.518	1.525	57	60	5.6243E+07	7.355E+06	13.077	1.688
Th232	1.2251E-01	8.802	2.541	12	12	1.2250E-01	1.078E-02	8.802	2.541

Typical data readout from the GV ICP-MS which includes the name of the element, the mean (after), standard deviation % (after), standard error % (after), included, and total. The total is the number of accumulations read and included indicates how many of those accumulations were averaged in to the (after) data, evaluated by 2 sigma. The mean (before), std dev, std dev % and std err % are data including all the accumulations before the 2 sigma evaluation.

The data from the readout was transferred into an Excel spreadsheet. For each element, the mean of the 5 replicates were averaged and the standard deviation and percent relative standard deviation were calculated. Once this was performed for both the background of Ar gas flowing through the sample cell and the ablated sample, they were subtracted from one another and the standard deviation and RSD again calculated for the background subtracted signal. The standard deviation was calculated using error propagation.

To calculate the concentration for the sample using one standard, the signals and concentration were ratioed to each other. All concentrations are given in weight % oxide unless otherwise stated. For percent difference calculations, the true concentration was subtracted from the calculated concentration then divided by the true concentration and multiplied by 100 percent.

For concentration calculations based on the 5 standards, a calibration curve was constructed and the value of the concentration was solved using the line slope equation from the calibration curve. For this data, the r^2 value is stated along with the true concentration, calculated concentration and percent difference between the true and calculated concentrations.

For the ratios calculated for the various isotopes, the signal from all the isotopes was summed and then each individual isotope signal was divided by the sum of all the isotopes signal. The ratio abundances were either compared to the true isotopic abundance or they were directly compared to each other and a percent difference was calculated. This was the simplest way to compare data between the samples.

6.0 RADIOACTIVE GLASS SAMPLES AND STANDARDS

6.1 RADIOACTIVE AY-102 GLASS

The radioactive AY-102 (hot) glass spiked with scandium oxide and used for Phase II work was made in the shielded cell facility of SRNL by Charles Coleman.[10] A bottle of a known amount of Sc_2O_3 was placed into the cells and a known amount of ground AY-102 glass powder was transferred into the bottle with the Sc_2O_3. Scandium was chosen as the internal standard so it had to be added to the composition of the AY-102 sample. This mixture was capped and mixed by manipulator shaking for 5 minutes. After the fines settled, approximately one minute, the mixture was transferred to a pre-weighed Pt-Au crucible. The mixture was vitrified for about 3 hours at 1100 degrees C, then cooled and weighed. The muffle furnace was re-equilibrated to 450 degrees C and the glass annealed for 1.5 hours. The starting mixture for this crucible vitrification weighed 8.7385 g and the final glass containing the incorporated Sc_2O_3 weighed 8.699 g. Thus a very small amount of 0.0395 g mass was lost during the vitrification process. The total amount of elemental Sc in the sample was calculated to be 2.9 wt%, or 4.44 wt% Sc_2O_3. The glass wafer was removed and placed into a plastic bottle for temporary storage.

6.1.1 Glass Radioactivity

According to previous RPP HLW glass analysis,[11] averaged total alpha measurements were 7.74E+01 μCi/g and total beta measurements were 3.92E+04 μCi/g. These measurements, Table 1 from Schumaker, et al.[11], were based on previous AY-102/C-106 glass that contained higher cesium content than the current AY-102/C-106, which is higher in strontium. Because these calculations were made on data which contained more Cs-137 than the current glass, the current shielding could be considered more than what was actually necessary. Other RPP dose data[10] indicated that a 50 mg powder glass sample that was removed for XRD- analysis in the previous AY-102 glass study,[8] gave an unshielded extremity reading of 6 Rem/hr from the shielded cells exit reading. This measurement was taken directly on the outside of a plastic cap of an inverted shielded bottle. The sample dose was 'non-detect' at 30 cm whole body. Based on the information at the time, it was calculated that using ¼ inch tungsten shielding around the sample and keeping a 6 inch distance, for 0.5 gram of glass, the extremity exposure rate would be about 106 mR/hr.

To acquire a small piece of glass that would fit in the holder and a piece less than half a gram, the over 8 gram sample was double bagged and a hammer was used to break the glass into smaller pieces. Adhesive was placed into the bottom of the sample holder and a small piece of glass, weighing 0.12 grams, was mounted into the sample holder in the shielded cells via remote handling. When the sample contained in the shielded sample holder came out of the cells, a very low dose reading of 0.2 mR/hr was labeled on the outer containment plastic bag. This dose rate was measured by Radiological Control Operations personnel when the holder was removed from the shielded cells.

When the bagged sample holder was later measured in the laboratory where work was to take place, it measured at about 17mR/hr. This difference was seen possibly because of incorrect surveying (the detector was not directly held over the shielded sample). These readings also show that the measured extremity dose rates for the shielded 0.12 g of the AY-102 glass in the range of 0.2 to 17 mR/hr are indeed below the previously calculated value of 106 mR/hr for a 0.5 g piece of AY-102 glass.

6.2 ARG GLASS (HOT)

Also within the shielded cells, a sample of ARG (hot) standard was spiked with scandium using the same method previously stated.[10] The recipe was the same as the AY-102 sample, except the elemental Sc was calculated to be 3.0 wt%, or 4.60 wt% Sc_2O_3. The starting mixture for this ARG (hot) crucible vitrification weighed 8.3892 g and the final glass containing the incorporated Sc_2O_3 weighed 8.364 g. Thus a very small amount of 0.0252 g mass was lost during the vitrification process. This sample was also crushed using a hammer and a small piece weighing 0.21 grams was mounted into the holder via remote handling in the shielded cells. Because this sample contained no radioactivity (other than the potential contamination from remote handling inside the shielded cells), the only concern was the sample shape and size for it to fit into the holder. This sample is referred to as hot ARG.

6.3 STANDARDS

Five non-radioactive glasses that encompassed the range of the composition of the simulant AY-102 were developed to be used as standards.[6,7] These glasses were the same standards that were used in Phase I and contained all of the elements requested for analysis in the statement of work and the task plan (except Th and U) and an internal standard, Sc. The composition of the standards can be found in Table 4. Once made, the standard compositions were confirmed by digestion and subsequent ICP-AES analysis,[7] but have not been through any round robin analyses. Along with the standards, simulant AY-102, AZ-101 and ARG were also made and contained scandium. These samples were used during analysis as “unknowns” for data comparisons.

One issue with these standards for use with the ICP-MS is that many of them are very high in concentration and saturate the detector. With the ICP-AES, only three of the elements saturated the detector at their highest concentration; however, it does appear that the higher concentrations for some of the elements may be out of the linear dynamic range of the instrument. Neither time nor budget permitted a study of the standards with the ICP-AES or -MS to determine if this was true or not.

Table 4. Composition of the RPP Standards (wt% oxide) and other non-radioactive samples (wt% oxide) all containing about 5% Sc_2O_3

	Avg RPP1	Avg RPP2	Avg RPP3	Avg RPP4	Avg RPP5	Avg AY-102	Avg AZ-101	Avg ARG
Al2O3	2.12	1.46	3.92	6.27	1.42	4.92	7.47	4.56
B2O3	8.74	5.77	4.98	3.70	14.69	9.67	10.34	7.86
CaO	2.12	2.61	1.03	0.55	0.14	0.49	0.48	1.39
Cr2O3	0.10	0.33	0.06	0.17	0.05	0.12	0.10	0.09
Fe2O3	9.32	5.01	7.10	3.87	19.63	12.90	11.08	13.51
K2O	1.03	0.11	1.92	3.99	0.11	0.02	0.16	2.39
Li2O	1.99	0.22	1.07	4.91	0.21	2.53	3.68	3.04
MgO	0.90	1.76	1.38	0.48	0.04	0.13	0.10	0.78
MnO2	4.86	1.12	6.43	0.00	0.00	3.24	0.22	2.12
Na2O	13.24	9.37	8.35	7.17	20.06	12.39	12.17	11.19
NiO	1.32	2.62	0.87	0.38	0.01	0.27	0.37	0.89
P2O5	0.71	1.31	0.62	0.43	0.21	0.49	0.36	0.23
Sb2O3	0.85	2.36	1.56	0.55	0.10	0.06	0.00	0.01
SiO2	35.85	54.90	41.03	45.93	37.10	46.16	44.82	45.93
SO4	0.17	0.30	0.15	0.23	0.09	0.21	0.16	0.09
SrO	1.93	0.20	3.83	6.78	0.20	0.15	0.16	0.01
TiO2	1.94	0.91	2.90	0.11	0.10	0.20	0.01	1.02
ZnO	2.98	0.90	4.08	0.10	0.10	0.65	1.97	0.03
ZrO2	2.37	0.06	1.62	6.23	0.09	0.01	0.02	0.14
Sc2O3	4.97	4.85	4.94	4.95	4.91	4.96	5.13	4.88
CdO	0.61	1.86	1.51	0.45	0.04	0.00	0.54	0.00
Tl2O3	0.28	0.81	0.42	0.26	0.00	0.00	0.00	0.00
BaO	0.00	0.00	0.00	0.00	0.00	0.08	0.07	0.08
Bi2O3	0.00	0.00	0.00	0.00	0.00	0.00	0.00	0.00
CeO2	0.00	0.00	0.00	0.00	0.00	0.07	0.17	0.00
CuO	0.00	0.00	0.00	0.00	0.00	0.04	0.04	0.01
La2O3	0.00	0.00	0.00	0.00	0.00	0.06	0.20	0.00
MoO3	0.00	0.00	0.00	0.00	0.00	0.03	0.00	0.00
Nd2O3	0.01	0.00	0.02	0.01	0.00	0.00	0.18	0.00
PbO2	0.00	0.00	0.00	0.00	0.00	0.48	0.07	0.00
PdO	0.00	0.00	0.00	0.00	0.00	0.00	0.00	0.00
RhO2	0.00	0.00	0.00	0.00	0.00	0.00	0.00	0.00
RuO4	0.00	0.00	0.00	0.00	0.00	0.00	0.00	0.00
SnO2	0.00	0.00	0.00	0.00	0.00	0.00	0.00	0.00
V2O5	0.00	0.00	0.00	0.00	0.00	0.00	0.00	0.00

Concentrations, in weight percent oxide, of the RPP standards and simulant glasses containing all the elements required by WTP for analysis. These glasses are non-radioactive.

7.0 LA-ICP-MS DATA

7.1 BARIUM ISOTOPES

The barium isotopes, masses 134-138, were monitored in the AY-102, AZ-101 and ARG samples. A cup was aligned for each of these masses to be monitored at the same time. Figure 2 shows the signal resulting from the ablation of the hot AY-102 sample. Although the x axis shows all of the peaks lined at mass 134, each of the different colored lines does represent the various isotopic masses. The yellow "AX" line (second from the bottom) is the center mass to which everything is referenced. The MS software allows the user to align the cups representing different masses atop one another for ease of monitoring. The greatest signal, the purple line, H4 (top most line), is the most abundant (71.4%) isotope Ba 138. The second most abundant (11.2%) isotope is Ba 137, represented by the teal line, H3 (second line from top). The less abundant naturally occurring isotopes of Ba are shown as the red line, H2 (third line from top) at 7.8%, the blue line, H1 (fourth line from top) at 6.6% and the yellow line, AX (second line from bottom) at 2.4%. The dark yellow line, L2, (very bottom) represents mass 133.

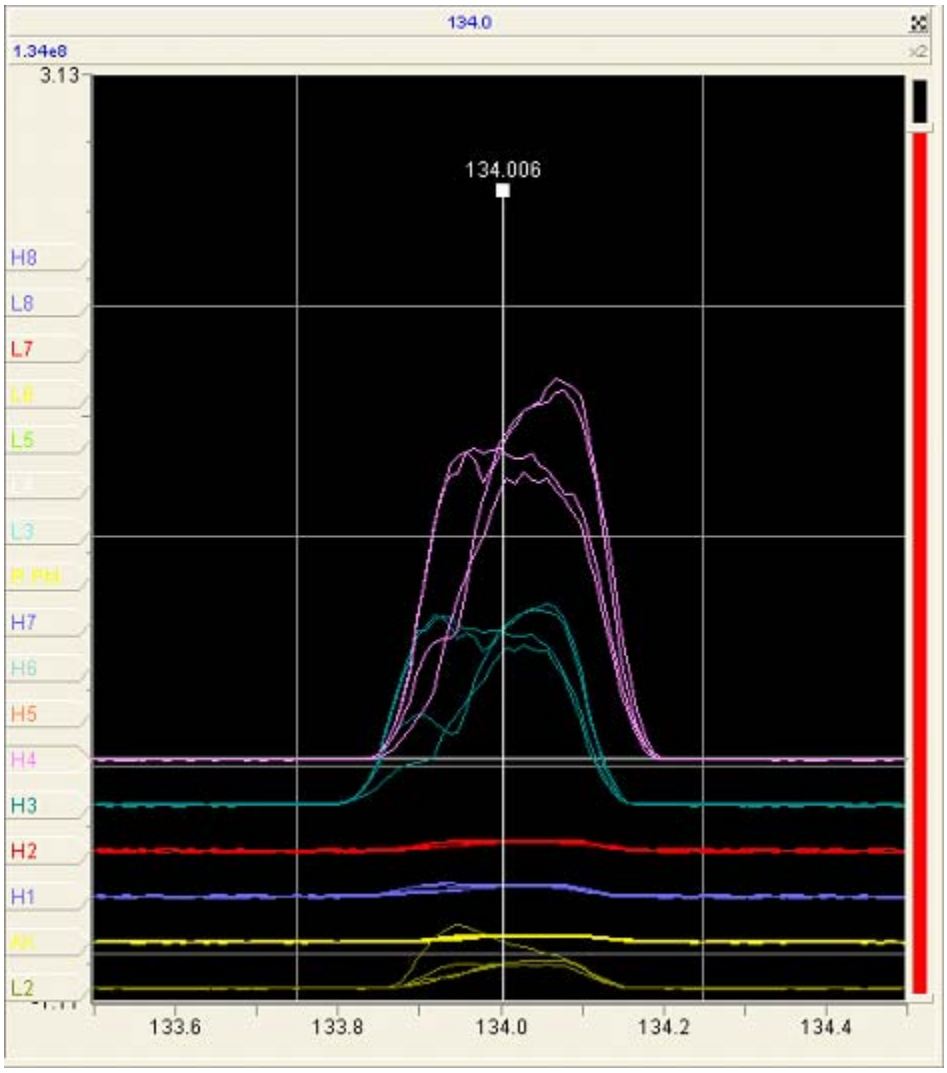

Figure 2. Plots of individual isotopes of barium

Isotope	Line identifier	Line color	Natural abundance
Ba 138	H4	Purple	71.70
Ba 137	H3	Green	11.20
Ba 136	H2	Red	7.85
Ba 135	H1	Blue	6.59
Ba 134	AX	Yellow	2.42
133	L2	Dark yellow	

The table indicates the isotope, line identifier, color on the figure and natural abundance ratio of the Ba isotopes.

Background signal, Ar flowing through the ablation cell, was subtracted from the ablation signal of each sample. The resultant signal was averaged for each sample and the standard deviation calculated, as well as the % RSD. The % RSDs for the AZ-101, ARG sample made on the bench top (cold), hot ARG sample (made in the shielded cells), two trials of the hot AY-102 sample, as well as the results from the dissolution of hot AY-102 performed at a previous time,[8] can be found in Table 5. Also in Table 5, the measured weight percent oxide of barium for each sample is shown on the bottom row of data. The weight percent oxide of the AZ-101 and ARG (cold) were confirmed previously,[7] the AY-102 (hot dissolution) was measured by the PQ2 ICP-MS,[8] while the ARG (hot) and AY-102 (hot) samples are based on weights from mixing calculations.[10] All samples contain the Sc except the original hot dissolution AY-102 sample. Percent RSDs for these samples range from 1 to 18%.

Table 5. LA-ICP-MS % RSD for barium isotopes of various samples

isotope	AZ101	ARG	ARG	AY102-1	AY102-2	AY102
		(cold)	(hot)	(hot)	(hot)	(hot dissolution)
Ba134	17	1	18	10	16	6
Ba135	17	1	18	15	17	1
Ba136	17	1	18	11	17	1
Ba137	17	1	18	11	16	2
Ba138	17	1	18	11	16	2
wt% Ox	0.07%	0.08%	0.09%	(0.06%)[1]	(0.06%)[1]	0.06%

1. ( ) weight % oxide based on measured weight calculations

Table 6 shows the calculated ratios of the Ba isotopes compared to their naturally occurring isotopic abundance ratios. The top three data sets are for non-radioactive glass. As a comparison, two sets of LA on hot AY-102 glass and a dissolution sample of hot AY-102 glass (values ratioed from Table A-1) are listed in the bottom three data sets. For the AZ-101 and ARG samples, which are non-radioactive samples, the percent difference between the calculated ratios and the true ratios are very good for all five of the Ba isotopes presented. The radioactive AY-102 (hot) ratios, however, have very high percent differences for masses 137 and below. An obvious reason for this would be that this is not naturally occurring Ba. Another reason for these high percent differences is due to the interferences of other radioactive isotopes within the sample. For instance, the 137 mass is higher due to the contribution of Cs-137, which is a main fission product along with Sr-90 from the original fissioning processes in the Hanford reactors. As an example, see Figure 4-18 in Friedlander et al.,[12] the uranium and plutonium fission product mass distributions that produce a bimodal distribution of fission products centered around atomic number 90 and 137.[13] These fission products make up the high level waste sludge slurry that was characterized[4] and vitrified[8] at SRNL to produce the hot AY-102 glass used for this study.

Table 6. LA-ICP-MS % difference calculation for the natural abundance ratios versus the measured and ratioed values

	natural Ba ratio	AZ 101	% diff	ARG cold	% diff	ARG hot	% diff
Ba134	2.42	**2.28**	-6	**2.34**	-3	**2.34**	-3
Ba135	6.59	**6.32**	-4	**6.44**	-2	**6.46**	-2
Ba136	7.85	**8.00**	2	**7.78**	-0.9	**7.80**	-0.7
Ba137	11.2	**11.18**	-0.1	**11.32**	1	**11.32**	1
Ba138	71.7	**72.21**	0.7	**72.12**	0.6	**72.07**	0.5
						AY102 hot	
	natural Ba ratio	AY102hot1	% diff	AY102hot2	% diff	dissolution	% diff
Ba134	2.42	**0.56**	-77	**0.59**	-76	**3.85**	59
Ba135	6.59	**1.11**	-83	**1.21**	-82	**1.17**	-82
Ba136	7.85	**0.80**	-90	**0.91**	-88	**1.07**	-86
Ba137	11.2	**22.20**	98	**22.04**	97	**21.27**	90
Ba138	71.7	**75.33**	5	**75.25**	5	**72.65**	1

The first column is the Ba natural abundance ratio followed by a sample and its abundance ratio and the percent difference between the two samples.

Despite these high percent differences of the mass numbers 137 and lower, in the hot AY-102 data shown in the bottom three data sets of Table 6, the isotopic ratios between the hot AY-102 samples using different sample introduction methods, i.e., LA vs. dissolution, are very similar, as shown in Table 7. Using the data from Table 6, Table 7 compares the various mass signals from the 'AY-102 hot1' versus the 'AY-102 hot dissolution' (first column of data) and also compares the 'AY-102 hot 2' versus the 'AY-102 hot dissolution' (second column of data). Although the Ba-134 and Ba-136 signals were somewhat lower in the LA versus the dissolution, the other mass number comparisons (mass 135, 137 and 138) are in good agreement when comparing the LA data and the dissolution data. Looking at the isotopic ratios for barium from the LA data on hot AY-102 and the dissolution data on hot AY-102 from Table 6 and Table 7, the laser ablation method is producing accurate results compared to the dissolution method. Recall that the only difference in the hot AY-102 glass sample that was laser ablated versus the original dissolved hot AY-102 glass was the inclusion of the small 4.47 wt% amount Sc_2O_3 into the laser ablated glass.

Table 7. Percent difference between Ba isotopic ratios for the AY-102 which was laser ablated and another which was dissolved

Isotope	% diff hot 1 vs. dissolved	% diff hot 2 vs. dissolved
Ba 134	-85	-85
Ba 135	-5	4
Ba 136	-25	-15
Ba 137	4	4
Ba 138	4	4

7.2 SOLVING FOR Cr, Zn, Sb, AND Mn IN THE RADIOACTIVE AY-102 SAMPLE

Due to time constraints and instrument constraints, only Cr, Zn, Sb, and Mn were analyzed in the radioactive AY-102 (hot) sample and compared only to the RPP #3 standard. Both modes of counts per second (CPS) and voltage (V) were used to collect the data. It is not clear how the software converts the volts to the CPS, and, from the data collected, no clear conclusions can be drawn (probably due to the somewhat irregular ablation process and power issues with the laser ablation). The background subtracted signal and relative standard deviation percentages for the standard and radioactive AY-102 sample (hot) are shown in Table 8. As stated previously, the radioactive piece of AY-102 (hot) glass that was sampled was not very flat and it was difficult to find a place to focus in to ablate. Most of the higher % RSDs can be seen for the radioactive AY-102 (hot) sample.

Table 8. Background subtracted readout and % RSD for CPS and V readings of the data (std=RPP #3 standard and hot=hot AY-102 sample)

Element	CPS	% RSD (for CPS)	Volts	% RSD (for V)
Cr std	6.24E+07	10	0.96	8
Cr std	7.64E+07	22		
Cr hot	2.11E+08	79	5.38	15
Cr hot	1.85E+08	46		
Mn std	1.04E+08	14	6.41	2
Mn std	8.14E+07	17		
Mn hot	3.14E+08	32	5.00	24
Zn std	1.38E+07	14	2.26	4
Zn hot	3.87E+07	38	0.63	31
Zn AY-102 (cold)			0.51	4
Sb std	3.76E+08	6	5.58	8
Sb hot	4.49E+05	17	0.006	16

Concentration calculations for all of the data were performed by ratioing the concentration and signal of the known standard to the signal of the AY-102 (hot) sample. For each element, the wt % oxide concentration of the specific element in the standard, the wt % oxide concentration of the radioactive AY-102 (hot) based on weight composition, the calculated wt % oxide concentration compared with the known standard, and the percent difference between the true and calculated value are reported.

7.2.1 Chromium

Chromium, mass 52, with a wt % oxide based concentration of 0.21% in the radioactive AY-102 (hot) sample (this was based on the original composition of AY-102[8] including a Sc spike- this was not verified by measurement with ICP-AES or MS) was compared to the RPP #3 standard containing 0.06 wt% oxide Cr_2O_3. There are four calculated concentrations of Cr in Table 9, because both the standard and sample were measured twice which made for a combination of four calculations. However, when summing both the standard and hot sample readings, the concentration averaged to be 0.17 wt % oxide with a percent difference of -18%, indicating the average calculated value of 0.17 wt% is slightly lower than the true value of 0.21 wt%. When using the voltage measurements to calculate the concentration, there is a percent difference of 60% for the calculated concentration of 0.34 wt % oxide. This difference could be explained by the sample issue of uneven surface of the radioactive AY-102 (hot) sample.

Previously in Phase I, both the RPP #3 standard and a sample of AY-102 (non-radioactive-cold) were analyzed with laser ablation on the Perkin Elmer Optima ICP-AES system (PE ICP-AES). Looking at the Cr background subtracted signal for the non-radioactive AY-102 sample and the RPP #3 standard, the concentration calculated using the same ratioing technique is 0.18% weight percent with a 51% difference between the true and calculated value (see next to last row of data in Table 9.) Using this ratioing technique, the LA-ICP-MS results for the radioactive data in CPS were better (18% difference in measured versus true concentration) than that with the cold LA-ICP-AES data (51% difference in measured versus true concentration.)

Also, the dissolution of radioactive AY-102 samples were analyzed on the JY 170C ICP-AES[8] (these samples will be called hot CC AY-102). These samples did not contain the Sc standard that is in the Phase II samples. Therefore, to directly compare the results obtained by LA-ICP-MS to the ICP-AES data, the Sc had to be backed out of the calculated concentration of the AY-102 sample. The ICP-AES measured concentration of Cr in the hot CC AY-102 sample was 0.20 wt % oxide. The calculated concentration of the radioactive AY-102 sample with the Sc backed out would be 0.18 wt% oxide. The difference between the ICP-AES and LA-ICP-MS measurement of the AY-102 sample was 11 percent. Therefore, as was the case when comparing the LA data on hot AY-102 and dissolved data on hot AY-102 for the barium isotopes in the previous section, similar comparisons using chromium indicate that there is indeed good agreement between the direct LA-ICP method and the dissolved glass data.

Table 9. Calculated concentration of Cr-52 for AY-102 and % difference

Mode	Element (λ-nm)	RPP Std #3 conc[a] (wt% oxide)	True AY-102 conc (wt% oxide)	Calculated AY-102 conc using std (wt% oxide)	% diff
CPS	Cr	0.06	0.21[b]	0.20	-3
CPS	Cr	0.06	0.21[b]	0.17	-21
CPS	Cr	0.06	0.21[b]	0.18	-15
CPS	Cr	0.06	0.21[b]	0.15	-31
Avg CPS	Cr	0.06		**0.17**	**-18**
Volts	Cr	0.06	0.21[b]	0.34	60
ICP-AES (PE)	Cr-267 nm	0.06	0.12[a]	0.18	51
ICP-AES (JY)	Cr-205 nm		0.20[c]	0.18[d]	-11

a. Concentration from dissolution performed by PS&E[7]
b. AY-102 (hot) concentration based on weight composition
c. JY ICP-AES measured concentration of hot CC AY-102 sample[8]
d. LA calculated radioactive AY-102 (hot) concentration taking out the Sc concentration

7.2.2 Manganese

Manganese, mass 55, was more difficult to measure and quantify because its high concentration caused the ICP-MS detector to saturate. The power on the LA unit was decreased and the spot size and raster size pattern were changed to allow the MS system to collect the data without saturating. The power was turned very low, to an output of 20% which barely registered 0.03 mJ on the LA unit energy meter. (In hind sight, this should have been explored more to allow the power to have more stability and improve the signal of the Mn.) The spot size was 100 microns with 50 microns between raster patterns. The percent difference is so high for this sample simply because the power was not stable. Percent RSDs for the AY-102 (hot) sample ranged up to 32% as can be seen in Table 8. The calculated concentration is very high compared to the small oxide wt % of 2.71%. This, therefore, leads to high percent differences as can be seen in Table 10. Again, the concentration was measured twice in the CPS mode, but neither of the calculated concentrations were close to the real concentration of the radioactive AY-102 (hot) sample. The voltage measurement was closer to the true concentration but still up to 85 % different.

When comparing the PE LA-ICP-AES data for the non-radioactive sample of AY-102 and RPP #3 standard, there is only a 27 % difference calculated. This is most likely due to the more stable ablation achieved using the Cetac laser ablation system and full power. Comparing the data obtained from the hot CC AY-102 sample and the radioactive AY-102 (hot) sample with the Sc backed out, there is a large difference of 549%. The calculated concentration is much higher than the true concentration.

Table 10. Calculated concentration of Mn-55 for AY-102 and % difference

Mode	Element	RPP Std #3 conc[a] (wt% oxide)	AY-102 conc (wt% oxide)	Calculated AY-102 conc using std (wt% oxide)	% diff
CPS	Mn	6.43	2.71[b]	19.33	613
CPS	Mn	6.43	2.71[b]	24.79	815
Volts	Mn	6.43	2.71[b]	5.01	85
ICP-AES (PE)	Mn-260 nm	6.43	3.24[a]	4.11	27
ICP-AES (JY)	Mn-257 nm		3.11[c]	20.19[d]	549

a. Concentration from dissolution performed by PS&E[7]
b. AY-102 (hot) concentration based on weight composition
c. JY ICP-AES measured concentration of hot CC AY-102 sample[8]
d. LA calculated radioactive AY-102 (hot) concentration taking out the Sc concentration

7.2.3 Antimony

Antimony, mass 121, was another one of the elements that saturated the ICP-MS detector so the power had to be turned lower. For these measurements, the power was at 50%, registering about 0.5 mJ, while the spot size again was only 100 microns with 50 microns between raster patterns. On the original AY-102 composition sheet for the calculated wt % oxides, Sb was not listed; however, it was known that there was some small amount contained in the sample. Because of this, the 0.0013% dissolution calculation from PQ2 ICP-MS results of the hot CC AY-102 sample was used (see Appendix A, Table A-1, mass number 121 (57.3% Sb abundance) and mass number 123 (42.7% Sb abundance)). As seen in Table 11, the calculated concentration from LA-ICP on the hot AY-102 sample was 0.0019 wt %. Thus the LA-ICP value is 43% higher than the concentration based on the dissolution data. For the volts mode, the LA-ICP value is 37% higher which is similar to the CPS mode measurement. If the amount of Sc in the AY-102 (hot) sample was added into the hot CC AY-102 measured concentration, its new concentration would be 0.0012 wt % oxide (CC AY-102 with Sc). The percent difference for CPS would then increase to 50% and the voltage percent difference would increase to 43%. This calculation is only weight based and was never created to be measured. Thus as seen in both the barium and chromium data presented earlier, there appears to be reasonably good agreement between the LA-ICP-MS direct analysis method and the dissolved hot AY-102 PQ2 ICP-MS data for the trace antimony that is in the glass.

For the 0.06 wt % Sb of the cold AY-102, data was compared to the calculated 0.0024 wt % using numbers from the PE LA-ICP-AES. This comparison shows the LA-ICP method giving a value that is 96% lower than the PE ICP-AES method. The Sb 206 nm reading is the data that was used when reporting the elements for the Phase I work. This line was used because it was the stronger signal of the two lines and had no interferences. However, when the radioactive JY ICP-AES was run, the line that was chosen to analyze for analysis was Sb 217 nm. When using the data from that line to recalculate the concentration, the calculated concentration of 0.04 wt% is only 30% lower than the 0.06 wt% value. One particular problem with the comparison of results from the LA-ICP-MS and the ICP-AES is that the AES instrument is not as sensitive. The numbers from the AES could possibly be close to noise for this very low level of antimony in the glasses, probably a reason why the percent difference is so drastically high for the 206 nm line. When comparing the radioactive JY ICP-AES data of 0.076 wt % oxide to the calculated concentration with the Sc taken out, 0.0019 wt %, the difference is -97%. Again, this high difference could be due to sensitivity issues with the AES system.

Table 11. Calculated concentration of Sb-121 for AY-102 and % difference

Mode	Element	RPP Std #3 conc[a] (wt% oxide)	AY-102 conc (wt% oxide)	Calculated AY-102 conc using std (wt% oxide)	% diff
CPS	Sb	1.56	0.0013[b]	0.0019	43
Volts	Sb	1.56	0.0013[b]	0.0018	37
ICP-AES (PE)	Sb-206 nm	1.56	0.06[a]	0.0024	-96
ICP-AES (PE)	Sb-217 nm	1.56	0.06[a]	0.04	-30
ICP-AES (JY)	Sb-217 nm		0.076[c]	0.0019[d]	-97

a. Concentration from dissolution performed by PS&E[7]
b. Concentration based on dissolution data from PQ2 ICP-MS of AY-102
c. JY ICP-AES measured concentration of hot CC AY-102 sample[8]
d. LA calculated radioactive AY-102 (hot) concentration taking out the Sc concentration

7.2.4 Zinc

Like antimony and manganese, zinc, mass 66, saturated the ICP-MS detector during laser ablation. The power on the laser ablation system was turned to 40%, which measured about 0.4 mJ and the diameter of the laser spot was decreased to 100 μ with 50 μ between raster patterns. Table 12 shows the results for the calculated wt % oxide concentrations of Zn, mass 66. For both the CPS mode and the volts mode, the calculated concentrations based on the LA-ICP-MS measurements about 15-16% higher than the AY-102 hot concentrations based on weight composition.

When the cold PE LA-ICP-AES data was compared the same way, the calculated concentration from LA-ICP-MS was 0.85 wt % oxide compared to the true AY-102 weight % oxide of 0.65 measured at 202 nm. So the LA-ICP-MS value was 30% higher than the cold PE LA-ICP-ES method.

Comparing the radioactive dissolution data set from the JY ICP-AES at 213 nm to the calculated LA concentration with the Sc removed, a difference of 69% was calculated. Thus the calculated concentration was 69% greater than the reported values from the JY ICP-AES.

Lastly for Zn, the non-radioactive AY-102 sample used for cold studies on the PE LA-ICP-AES was analyzed. It was compared two ways: the RPP #3 standard was used and compared to the non-radioactive AY-102 sample (footnote [e.] on Table 12) and the non-radioactive and radioactive AY-102 (hot) samples were compared (f. on Table 12). RPP standard #3 with a measured concentration of 4.08 wt % oxide and measured (voltage) signal was compared with the measured (voltage) signal of the non-radioactive AY-102 sample. The calculated concentration was 0.93 wt %, which is a difference of 43% from the true value. In comparison, the non-radioactive AY-102 with a measured concentration of 0.65 wt % was compared to the (voltage) signal of the radioactive AY-102 (hot) sample. This concentration was calculated to be 0.80 wt %, a difference of only 19%. Due to time constraints, only the voltage mode was measured for the Zn sample for the non-radioactive AY-102 sample.

Table 12. Calculated concentration of Zn-66 for AY-102 and % difference

Mode	Element	RPP Std #3 conc[a] (wt% oxide)	AY-102 conc (wt% oxide)	Calculated AY-102 conc using std (wt% oxide)	% diff
CPS	Zn	4.08	0.99[b]	1.14	15
Volts	Zn	4.08	0.99[b]	1.15	16
ICP-AES (PE)	Zn-202 nm	4.08	0.65[a]	0.85	30
ICP-AES (JY)	Zn-213 nm		0.71[c]	1.19[d]	69
Volts	Zn- AY102[e]	4.08	0.65[a]	0.93	43
Volts	Zn- AY102[f]	0.65[a]	0.99[b]	0.80	-19

a. Concentration from dissolution performed by PS&E[7]
b. AY-102 (hot) concentration based on weight composition
c. JY ICP-AES measured concentration of hot CC AY-102 sample[8]
d. LA calculated radioactive AY-102 (hot) concentration taking out the Sc concentration
e. Treating RPP #3 (4.08 wt%) as standard and the non-radioactive AY-102 (0.65 wt%) as unknown
f. Treating non-radioactive AY-102 (0.65 wt%) as standard and the radioactive AY-102 (hot) (0.99 wt%) as unknown

7.3 LEAD AND THORIUM

Both Pb 208 and Thorium 232 were analyzed on the GV LA-ICP-MS. Unfortunately, no conclusions can be drawn from the data. Pb data, shown in Table 13 was taken on the AZ-101 sample, which had a concentration of 0.07 wt % oxide. During Phase I work with the PE LA-ICP-AES, it was difficult to detect some concentrations below 0.5 wt % oxide so data was not available for comparison. The signal could be seen, however, on the ICP-MS for this low concentration.

Thorium 232 was also measured using the GV LA-ICP-MS on the AZ-101 and radioactive AY-102 (hot) samples and the data can be seen in Table 13. With the hot CC AY-102 sample, dissolution data (PQ2-ICP-MS) states that there was a concentration of 0.064 wt % oxide (see Appendix A, Table 23, mass number 232). Using the same ratioing as previously used, the calculated Th 232 concentration in the AZ-101 sample would be 0.0005 wt % oxide. The true concentration of Th in the AZ-101 sample is unknown. However, from this calculation, it shows that there is a very small quantity. The RSD of the AZ-101 sample was 7%, while that of the radioactive AY-102 (hot) sample was 15%.

Scandium was also run quickly to determine the problems with the Sc-45 mass. The power on the LA system was turned to 50% due to saturation of the MS detectors. A high signal was obtained and the RSD was 33%.

Table 13. Background subtracted signal, standard deviation and % relative standard deviation in CPS for Pb, Th and Sc

Element and Sample	Signal-Bkg (CPS)	Std dev	%RSD
Pb-208 AZ-101	0.19	0.01	7
Th-232 AZ-101	0.00123	0.00009	7
Th-232 AY-102(hot)	0.16	0.02	15
Sc-45 AY-102(hot)	3	1	33

7.4 URANIUM ISOTOPES

Masses 233-242 were also analyzed by GV LA-ICP-MS. The U concentration of the radioactive AY-102 (hot) sample was unknown; however, data from previous dissolution of hot CC AY-102 was used for comparison. Table 14 shows data of the uranium isotopes 233-238. There were 3 replicates used in the PQ2-ICP-MS dissolution method (CC #), and they were treated as separate samples and not averaged. Data shown in Table 14 for the CC 1 – CC 3 samples can be found in Appendix A, Table A-1 , masses 233 – 238. The ratios for each isotope were calculated by dividing the individual isotopic signal by the sum of all the signals and multiplying by 100%. The natural abundance ratios fro the U isotopes are 99.3% for U-238, 0.72% for U-235 and 0.01% for U-234. Table 14 shows that the measured ratios agree well with the natural abundance ratios.

Table 14. Uranium isotope ratios for AY-102 (hot) and dissolution data (CC #)

mass	AY-102 signal	AY-102 ratio %	CC 1 µg/g	CC 1 ratio %	CC 2 µg/g	CC 2 ratio %	CC 3 µg/g	CC 3 ratio %
233	1.50E-04	**0.0145**	0.303	**0.0179**	0.43	**0.0250**	0.298	**0.0181**
234	6.42E-05	**0.0062**	0.121	**0.0072**	0.116	**0.0067**	0.119	**0.0072**
235	7.05E-03	**0.6802**	11.5	**0.6795**	11.7	**0.6792**	11.7	**0.7123**
236	2.98E-04	**0.0288**	0.502	**0.0297**	0.48	**0.0279**	0.535	**0.0326**
238	1.028	**99.270**	1.68E+03	**99.266**	1.71E+03	**99.261**	1.63E+03	**99.230**

Percent differences were calculated by comparing the radioactive AY-102 (hot) ratio percent to the individual CC ratio %, and results are displayed in Table 15. The GV LA-ICP-MS data showed lower ratioed values for mass 233 versus the dissolved PQ2 ICP-MS ratio, in the range of 19 to 42 % lower. However, for the other ratioed mass numbers, differences in the two methods were within about 15%. For the most prominent mass 238 peak, there was very good agreement between the two methods with differences of less than 1%. Comparing the LA data of the AY-102 to the true natural abundance of U isotopes shows that the 234 isotope agrees to within 38%, the 235 isotope to within 6%, and the 238 isotope to within 0.03%.

Table 15. Percent differences between Uranium isotope ratios of AY-102 (hot) and dissolution data (hot CC AY-102)

U mass	% diff w/ CC 1	% diff w/ CC 2	% diff w/ CC 3
233	-19	-42	-20
234	-13	-8	-14
235	0.10	0.15	-5
236	-3	3	-12
238	0.005	0.009	0.041

The same calculations can be made for the mass range 239-242. As discussed in the radionuclide analysis section of Reference 8, masses 239 and 240 are attributed to long-lived plutonium isotopes and mass 241 could be Pu-241 or Am-241. Mass 242 is attributed to both Pu-242 and Cm-242. Table 16 shows the results for the radioactive GV LA-ICP-MS AY-102 ratio calculations compared to the dissolution data of hot CC AY-102 by PQ2 ICP-MS. In this set of results, the ratio comparison of Mass 240 to Mass 239 is given for the radioactive AY-102 (hot) and the dissolution data (CC 1). The % difference between the two samples 240/239 ratio agrees to within 3% as shown in the final column of Table 16. Comparison of the % differences in the ratioed mass values between the GV ICP-MS and the PQ2 ICP-MS data shows good agreement (% differences from -0.4% to 15.3%) for masses 239 to 241 as shown in the next to last column of Table 16. The LA-ICP-MS value for mass 242 ratio indicates an 80% lower value than the hot CC AY-102 dissolution. However, one problem with this measurement is that for the hot CC AY-102 dissolution, the Pu 242 was at the instrumental detection limit. The number of 0.20 µg/g could be lower or higher and perhaps would have yielded a better percent difference if the true value was determined.

Table 16. Mass 239-242 ratio calculations

Mass number	AY-102 signal	AY-102 ratio %	Ratio 240/239	CC 1 µg/g	CC 1 ratio %	Ratio 240/239	% diff	% diff 240/239
239	0.02185	88.928	0.0712	30.9	89.255	0.0689	-0.4	3
240	0.00156	6.330		2.13	6.153		2.9	
241	0.00114	4.628		1.39	4.015		15.3	
242	2.80E-05	0.114		<0.2	0.578		-80.2	

7.5 CALIBRATION CURVES

To truly compare the results obtained by LA-ICP-MS to the work performed on the LA-ICP-AES, a calibration curve was generated for both Cr and Zn using the 5 RPP standards and analyzing the glasses ARG, AZ-101, and AY-102 and treating them as "unknowns." At this point, the radioactive AY-102 (hot) sample had to be returned to the cells for repackaging. This data does not contain any information on the radioactive material and contains a new set of data from the glasses. Two different plots were created using all of the calibration points and then only the concentration points that yielded the best slopes.

7.5.1 Chromium

Chromium was found in small concentrations of less than 0.11 wt % oxide in all of the "unknown" samples. However, as seen in Figure 3 from the experimental calibration curve data, sample signals did not fall into the linear trendline of the standards. It is possible that the calibration standards are not within the linear dynamic range of the instrument. It does appear that the regression line does start to curve over at the higher concentrations.

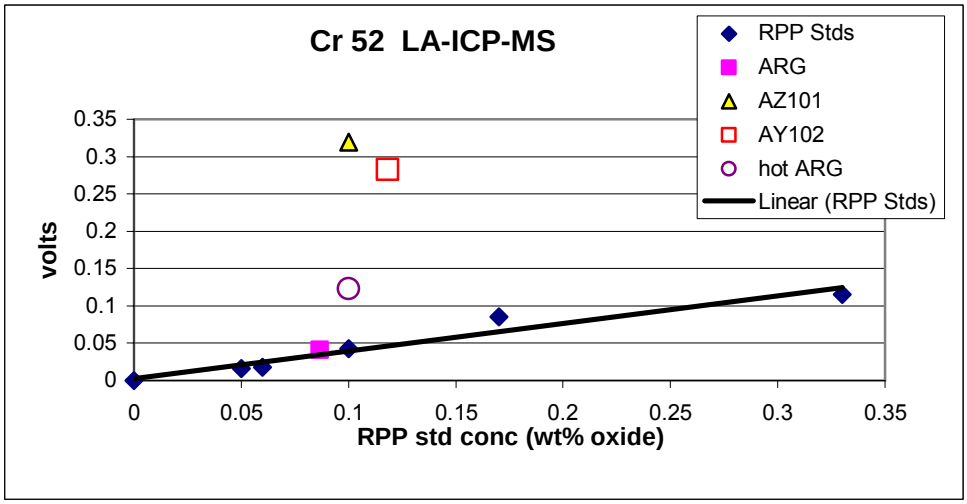

Figure 3. Graphical representation of the calibration curve of Cr and the signals of the samples

Because of this, percent difference calculations were extremely high, as seen in Table 17. This table shows the true concentration for each of the samples along with the concentration calculation from the calibration curve and the percent difference. The (hot) ARG is the sample that was made in the shielded cell, but did not contain any radioactivity. The designation of (hot) differentiates it from the sample that was made on the bench top. For comparison, data taken from PE LA-ICP-AES on various days is also presented. The only data that does agree is the ARG for both the LA-ICP-MS and –AES. Looking back at the MS data from Section 7.2, Table 8, it seems that the voltage measurements for this calibration data are not as high as they were in Table 8. Therefore, the fact that the samples readings are so high compared to the standards may mean that the instrument was having problems.

Table 17. Comparing LA-ICP- MS and -AES Cr calibration curve concentration calculations

		LA-ICP-MS				LA-ICP-AES	
Sample	Conc wt % ox	Calib Curve Calc Conc wt % ox	% diff		Conc wt % ox	Calib Curve Calc Conc wt % ox	% diff
AY-102	0.12	0.75	538		0.12	0.12	2
						0.10	-12
						0.08	-32
ARG	0.09	0.10	20		0.09	0.07	-17
						0.07	-20
						0.06	-29
(hot) ARG	0.10	0.33	226				
AZ-101	0.10	0.85	754		0.10	0.08	-25
						0.07	-29
						0.06	-39

7.5.2 Zinc

Like the previous Cr data, Zn was also analyzed and plotted in a calibration curve. The problem with Zn was that it had saturated the detector, and, in order to avoid this, either the Zn 66 or Zn 67 mass was measured. To get them both on the same scale, mass 67 was multiplied by 6.8, which is the factor corresponding to the natural abundance ratio chart of isotopes.

Table 18 shows the signal, standard deviation, % RSD and true concentrations (wt % oxides), and masses for the different samples measured in volts. The % RSDs for these samples are all under 10% except RPP #3. When the data from the table is plotted, see Figure 4, the last data point, RPP #3, curves over. When that point is left out of the calibration curve, the slope of the line is 0.978 versus 0.914. On the right side of that figure, the calibration plot for the LA-ICP-AES is shown. Except for the last data point on the LA-ICP-MS data, they both show similar trends.

Table 18. Zn data for calibration curve generation

Sample	True conc wt % oxide	S-B (V)	Std dev	% RSD	Mass
RPP #1	2.98	1.759	0.079	5	67
RPP #2	0.90	1.835	0.024	1	67
RPP #3	4.08	0.329	0.047	14	66
RPP #4	0.10	5.473	0.088	2	66
AY102	0.65	1.473	0.046	3	66
AZ101	1.97	1.162	0.052	4	67
(hot) ARG	0.02	0.083	0.003	3	66
ARG	0.03	0.048	0.004	8	66

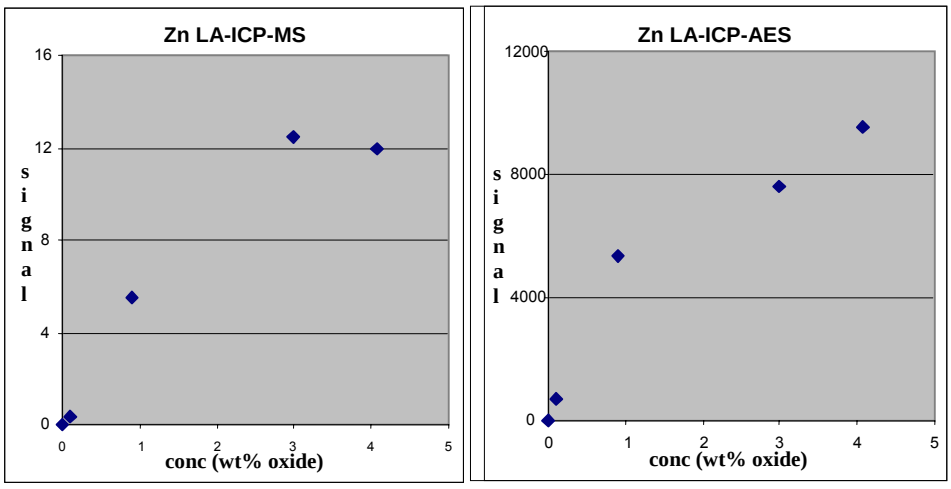

Figure 4. Calibration curves for Zn using LA-ICP-MS and -AES

Table 19 shows the concentration calculation for the Zn wt % oxide with various calibration points excluded. Along with the percent differences, the r^2 values for each of the calibration combinations are stated. For this data, a 0-4.08 wt % oxide concentration means that all points were included in the calibration and subsequent sample calculation. This is the plot from Figure 4. The 0-2.98 concentrations has excluded the last 4.08 concentration of the standard since it curves over in the plot and may indicate that it is out of the dynamic range of the instrument. For the next column, only the 0.1 and 3.08 concentrations are included in the calibration. This combination actually yields an r^2 value of 5 nines. Of all of the curves, this one probably has the best percent differences overall. Lastly, only the first two concentrations are plotted, 0.1 and 0.9. These also yield better percent differences than the others. When comparing the calibration curve plots in Figure 4, it would be easy to dismiss the last two concentration points as both of them do not follow the trend of the first several points.

Table 19. Calculated wt % oxide concentrations for Zn using various calibration curve combinations

	True conc	0-4.08 conc	% diff	0-2.98 conc	% diff	0,0.1,4.08 conc	% diff	0,0.1,0.9 conc	% diff
AY102	0.65	0.16	-75	0.25	-61	0.50	-24	0.26	-60
AZ101	1.97	2.20	12	1.79	-9	2.69	37	1.29	-34
hot ARG	0.02	0	-1478	0	-501	0.02	11	0.04	77
ARG	0.03	0	-1056	0	-395	0.01	-67	0.03	-1
r^2 value		0.914		0.978		1.000		0.998	

The data taken on the AES system was better than that taken with the MS system for the element of Zn. It is believed that these differences are instrument related, both laser ablation and detection. Table 20 shows the comparison data for the AES and MS systems. For this Zn data, the AZ-101 samples were the closest to each other probably because of its higher concentration.

Table 20. Comparing LA-ICP-MS and -AES Zn calibration curve wt % oxide concentration calculations

		LA-ICP-MS				LA-ICP-AES	
Sample	Conc wt % oxide	Calib Curve Calc Conc wt % oxide	% diff		Conc wt% oxide	Calib Curve Calc Conc wt % oxide	% diff
AY-102	0.65	0.16	-75		0.65	0.60	-7
						0.61	-6
						0.76	18
ARG	0.03	0	-1056		0.03	0	-387
						0	-1138
						0	-438
(hot) ARG	0.02	0	-1478				
AZ-101	1.97	2.20	12		1.97	1.69	-14
						2.05	4
						2.19	11

8.0 RPP STANDARDS STUDY

During the administrative and set-up process of the LA unit for radioactive work, the study of the use of 5 created standards for calibration continued. Some of the data collected during these studies was previously discussed as a comparison to the LA-ICP-MS data. The data in this section were all cold samples. All of the data collected used the Cetac LSX-200 for laser ablation and signal collection and analysis by the Perkin Elmer Optima 3000 ICP-AES. The following section will describe the results obtained from the continuation of this standards study.

8.1 CALIBRATION CURVE CONCENTRATION CALCULATION

Table 21 shows the calculated concentrations of the AY-102 (S) sample using the RPP standards for calibration. Within this table, the true concentration of S (wt % oxide), the calculated concentration (wt % oxide), the percent difference between the true and calculated concentrations, and the r^2 value generated from the calibration curve are seen. The element and wavelengths are listed in the first column of Table 21. The highlighted elements are the ones that have been chosen for monitoring because they have no interferences and usually have given the greatest and most reproducible signal. In this table, all of the data has been included to give the reader an idea of the amount of data that is analyzed, show the differences in concentration calculations for the various wavelengths, and the need to monitor several different wavelengths of the same element to ensure proper signal behavior.

Table 21. Solving for AY-102 (wt % oxide) using calibration curves

	S conc	calc conc	% diff	r^2 (a)		calc conc	% diff	r^2 (b)		calc conc	% diff	r^2 (c)
Al 396.153	4.92	3.66	-26	0.902		5.63	14	0.968		3.34	-32	0.809
Al 308.215	4.92	5.65	15	0.968		4.91	0	0.959		7.35	49	0.674
B 249.772	9.67	9.52	-2	0.940		9.78	1	0.987		8.79	-9	0.869
B 208.889	9.67	9.57	-1	0.945		9.82	2	0.989		8.83	-9	0.873
Ca 393.366	0.49	0.42	-14	0.957		0.51	4	0.998		0.41	-17	0.803
Ca 422.673	0.49	0.42	-15	0.957		0.50	2	0.999		0.40	-19	0.808
Cr 267.716	0.12	0.12	2	0.714		0.09	-24	0.939		0.12	2	0.930
Cr 357.869	0.12	0.17	41	0.976		0.16	36	0.998		0.15	31	0.950
Fe 238.204	12.90	13.98	8	0.950		14.39	12	0.997		12.36	-4	0.906
Fe 239.562	12.90	13.32	3	0.950		13.78	7	0.997		11.82	-8	0.907
Fe 259.939	12.90	13.35	3	0.950		13.82	7	0.997		11.85	-8	0.906
K 766.490	0.02	0.24	1507	0.932		0.02	36	0.999		0.29	1815	0.880
Li 670.784	2.53	2.01	-21	0.981		2.69	6	0.997		1.80	-29	0.941
Li 610.362	2.53	2.90	14	0.940		5.37	112	0.964		2.53	0	0.903
Mg 285.213	0.13	0.09	-33	0.935		0.13	-1	1.000		0.09	-28	0.800
Mg 280.271	0.13	0.10	-19	0.944		0.13	3	1.000		0.11	-14	0.808
Mn 257.610	3.24	3.45	6	0.997		3.45	6	0.997		3.36	4	0.906
Mn 260.568	3.24	3.36	4	0.997		3.36	4	0.997		3.27	1	0.906
Na 589.592	12.39	11.85	-4	0.889		12.95	5	1.000		11.22	-9	0.821
Na 588.995	12.39	11.88	-4	0.869		13.10	6	0.999		11.23	-9	0.805
Ni 231.604	0.27	0.28	7	0.966		0.36	36	0.985		0.30	14	0.903
Ni 232.003	0.27	0.28	7	0.965		0.36	36	0.985		0.30	14	0.903
P 213.617	0.49	0.38	-22	0.952		0.40	-19	0.999		0.38	-23	0.914
P 214.914	0.49	0.48	-2	0.925		0.49	1	0.998		0.46	-6	0.882
Sb 206.836	0.06	-0.06	-201	0.969		0.04	-37	0.990		-0.02	-138	0.857
Sb 217.582	0.06	-0.04	-169	0.966		0.06	-4	0.988		0.00	-107	0.852
Si 251.611	46.16	40.24	-13	0.799		50.58	10	0.998		40.19	-13	0.896
Si 288.158	46.16	39.13	-15	0.792		49.39	7	0.999		39.14	-15	0.893
S 180.669	0.21	0.12	-42	0.500		0.06	-70	0.984		0.13	-38	0.624
S 189.965	0.21	-0.13	-158	0.186		0.02	-89	1.000		-0.10	-146	0.179
Sr 407.771	0.15	0.48	215	0.913		0.15	2	1.000		0.55	261	0.842
Sr 421.552	0.15	0.41	171	0.943		0.15	2	1.000		0.49	224	0.866
Ti 334.940	0.20	-0.03	-115	0.983		0.03	-87	0.995		0.00	-101	0.872
Ti 336.121	0.20	0.09	-56	0.740		0.86	337	0.998		0.07	-62	0.613
Zn 213.857	0.65	0.61	-6	0.000		0.69	7	0.000		0.60	-8	0.000
Zn 202.548	0.65	0.60	-7	0.990		0.68	6	1.000		0.59	-9	0.889
Zr 343.823	0.01	0.24	2150	0.975		0.00	-60	0.996		0.33	3002	0.940
Zr 339.197	0.01	0.24	2142	0.975		0.00	-57	0.996		0.32	2997	0.940
Sc 361.383	4.96	4.83	-3	0.768		4.37	-12	1.000		4.92	-1	1.000
Sc 357.253	4.96	3.84	-23	0.373		3.74	-25	1.000		4.14	-16	0.688
Cd 228.802	0.00	-0.08	—	0.875		-0.05	—	0.970		-0.08	—	0.718
Cd 226.502	0.00	-0.08	—	0.885		-0.05	—	0.972		-0.08	—	0.727
Tl 190.801	0.00	-0.07	—	0.951		-0.01	—	0.998		-0.19	—	0.773
Tl 276.787	0.00	-0.07	—	0.941		-0.07	—	0.941		-0.19	—	0.766
Tl 351.924	0.00	-0.06	—	0.934		-0.06	—	0.934		-0.17	—	0.807

The first section of the data, (a) is using all of the standards in a calibration curve to generate the AY-102 concentration. Of the elements, 45% are under 10% RSD and 25% are under 20% RSD. In the second section, (b), are concentrations calculated by choosing the concentrations that generate the best calibration curve. The particular concentrations chosen either yielded the best r^2 value or all followed the same pattern without straying too far outside the approximated line estimate. In set (b) of data, there are many more elements that are under 10% RSD. All of the < 20% RSD improved to less than 10% RSD, with only one of the less than 10% RSD moving over to the <20% RSD column. Four of the original over 20% RSD elements (K, S, Ti, and Zr) still remain over 20% with some of them improving slightly. The last set of columns (c) shows the calculated concentrations when all of the data is ratioed to Sc. Scandium oxide was doped into all of the samples at a concentration of about 5%. It was hoped that this element could be used as an internal standard to improve the results. As seen from this set of data, the ratioing to Sc did not really improve the results. For this case, the over 20% RSD actually got worse compared to the calibration curves using all the points. The amount of elements that fit into this category was 35%. The <20% RSD improved slightly while the under 10%RSD stayed the same with only one element being different than the all points set of calibration data. This shows that perhaps only some elements would benefit from ratioing while others would not. The elements that always were under 10% RSD in all of the cases were B, Cr, Fe, Mn, Na, P, Zn and Sc.

Table 22 and Table 23 show calculations of B (249 nm) and Mn (260 nm), respectively, over different time periods. Within these tables, the calculated concentration using straight calibration data is compared with the same data except ratioed to the Sc 361 nm emission line. The first three columns after the number, show the calculated wt % oxide, % difference between the true concentration (bolded in parenthesis in the heading) and calculated concentration and the r^2 value for the calibration curve. The next three columns show that same data except ratioed to the Sc line. In some cases, upon ratioing, the % difference improved. Also for most of the data, upon ratioing the r^2 value increased as well. However, a good percent difference does not always indicate a good r^2 value. The majority of this information, a representation of 4 separate sets of data, shows that some of the elements analyzed may have to be ratioed when others will not. A thorough examination of the linear dynamic range of the ICP system would also help improve this data.

Looking at the B data, the r^2 slope values range from 0.651 to 0.940. Upon plotting this data over time, it is revealed that some of the concentrations do not increase as they should. As this sometimes happens with other sets of calibration data, it can only indicate that the sample is inhomogeneous and the position being ablated is higher in concentration. Another reason could be that the laser ablation system or ICP-AES was not properly working when that sample was run. Looking at other sets of data over time, it seems that this is a case of sample inhomogeneity. Although when looking at the plots of the signal over time, they do not reveal indication of spots higher in specific concentrations, it may be that the particular area is higher in an elemental concentration than another area.

Table 22. B (249 nm) concentration calculations using calibration curves and calibration curves ratioed to Sc from different days

B	Calc. AY-102 (**9.76** wt% ox)	%diff	r^2		Calc. AY-102 ratioed to Sc	%diff to Sc	r^2
1	10.16	5	0.651		9.75	1	0.944
2	12.26	27	0.885		9.15	-5	0.904
3	9.52	-2	0.940		8.79	-9	0.869
4	12.76	32	0.674		9.83	2	0.932
B	ARG (**7.86** wt% oxide)	%diff	r^2		Calc. ARG ratioed to Sc	%diff to Sc	r^2
1	7.23	-8	0.651		8.13	3	0.944
2	7.55	-4	0.885		7.49	-5	0.904
3	7.34	-7	0.940		7.16	-9	0.869
4	7.57	-4	0.674		8.12	3	0.932
B	AZ-101 (**10.34** wt% oxide)	%diff	r^2		Calc. AZ-101 ratioed to Sc	%diff to Sc	r^2
1	11.28	9	0.651		10.04	-3	0.944
2	13.86	34	0.885		9.49	-8	0.904
3	10.40	1	0.940		9.72	-6	0.775
4	13.34	29	0.674		10.21	-1	0.932

Table 23. Mn (260 nm) concentration calculations using calibration curves and calibration curves ratioed to Sc from different days

Mn	Calc. AY-102 (**3.24** wt% ox)	%diff	r^2		Calc. AY-102 ratioed to Sc	%diff to Sc	r^2
1	4.06	25	0.952		3.44	6	0.992
2	4.09	26	0.976		2.92	-10	0.989
3	3.36	4	0.997		3.27	1	0.906
4	5.11	58	0.960		3.61	11	0.980
Mn	ARG (**2.12** wt% oxide)	%diff	r^2		Calc. ARG ratioed to Sc	%diff to Sc	r^2
1	2.31	9	0.952		2.24	6	0.992
2	1.96	-7	0.976		1.85	-12	0.989
3	2.07	-2	0.997		2.09	-1	0.906
4	2.44	15	0.960		2.32	9	0.980
Mn	AZ-101 (**0.22** wt% oxide)	%diff	r^2		Calc. AZ-101 ratioed to Sc	%diff to Sc	r^2
1	0.11	-49	0.952		0.32	43	0.992
2	0.32	43	0.976		0.18	-20	0.989
3	0.25	12	0.997		0.204	-8	0.930
4	0.17	-24	0.960		0.30	37	0.980

8.1.1 Inhomogeneity

As stated above, an indication of sample inhomogeneity can be gained by reviewing the ablation profile of the elements over time. The question of sample homogeneity may always be an issue with laser ablation unless a sample preparation method can be developed that proves that the sample is homogenous. In the dissolution method, sample homogeneity is not as critical because the entire is dissolved and analyzed. With laser ablation, if a section of the glass is higher in one element than another and all that is ablated is that higher concentration, then the concentration calculations from the calibration curve would be inaccurate. It is therefore highly encouraged that several areas across the surface of a sample are analyzed. There are also techniques utilized, such as normalization, which aid in this issue.

The signal over time of some of the RPP standards can be seen in Figure 5 and Figure 6. The three elements that seem different from the other elements patterns are Li (green circle), Na (orange outline triangle), and Ca (maroon circle). This was the case with all of the RPP standards, as well as the samples, as seen in Figure 7. This monitoring does not aid in the case previously discussed where the entire concentration seemed to be incorrect. For that instance, the plots that reveal the best data will have to be compared with the data being taken and if something does not match, the sample will need to be run again.

There are other factors that can and will lead to signal fluctuations. These factors include the stability of the laser as well as mass ablation. Lasers have improved over the years with their power stability. However, over time and wear, it is possible that the power may have to be more carefully monitored to account for signal fluctuations. Power fluctuations can lead to mass ablation fluctuations which will certainly alter signal collection. Again, better monitoring of the power will aid in this determination. The size of the particles entering the ICP torch can also influence the signal collected.

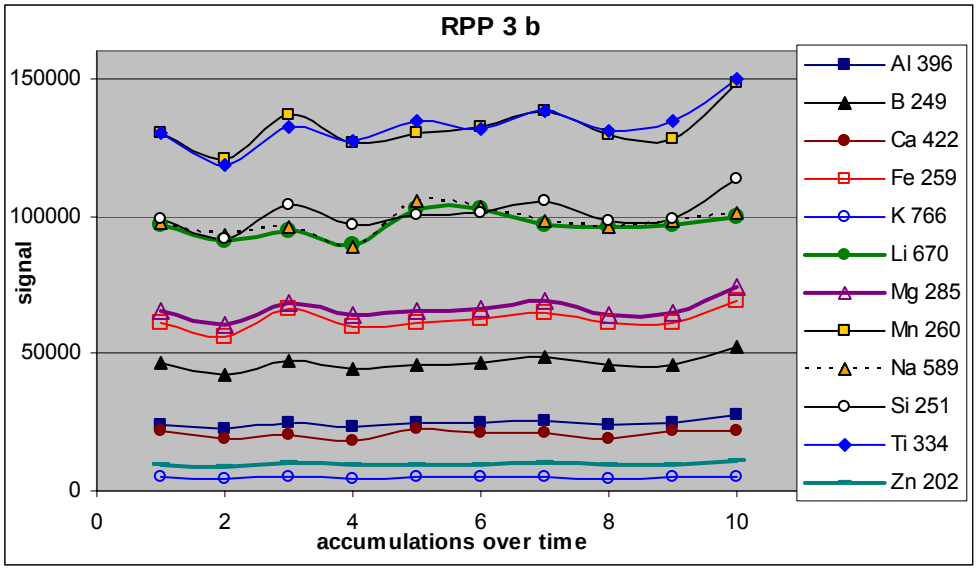

Figure 5. Signal over time for the elements in RPP standard #3

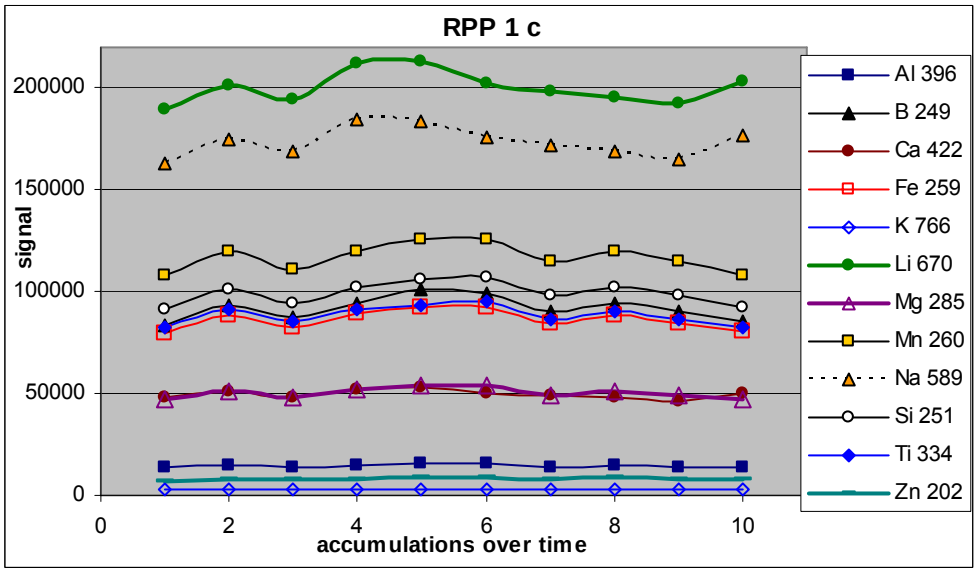

Figure 6. Signal over time for the elements in RPP standard #1

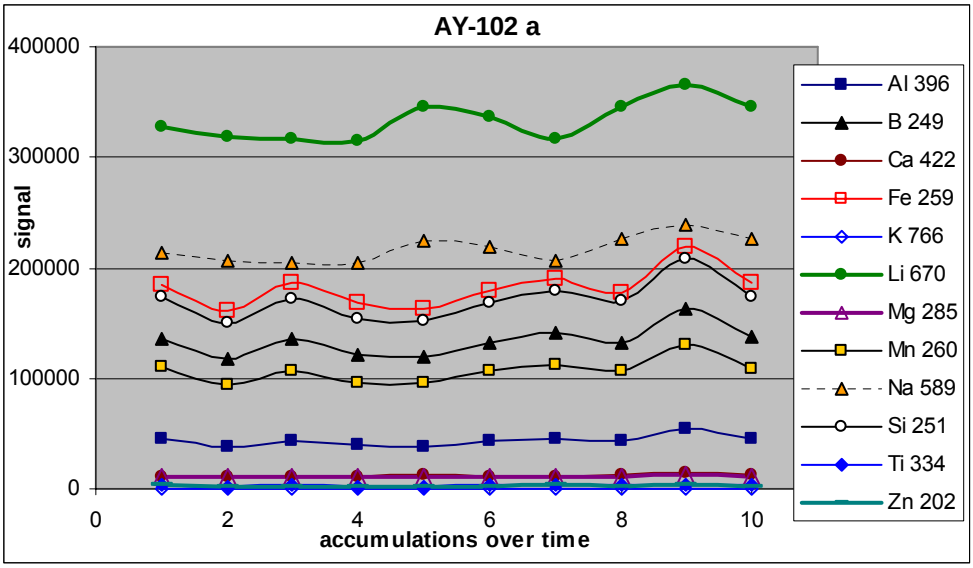

Figure 7. Signal over time for the elements in the (cold) AY-102 simulant sample

9.0 QUALITY ASSURANCE

The Quality Assurance measures identified in the Task Technical and Quality Assurance Plan[1] were followed in the performance of the Phase II activities. This involved following the WSRC Quality Assurance Program, which has been approved by WTP, and the WSRC Quality Assurance Management Plan (WSRC-RP-92-225). The WSRC program applies the appropriate quality assurance requirements from 10 CFR 830 Subpart A, NQA-1-1989 (Part I, Basic and Supplementary Requirements), and NQA-2a-1990, Part 2.7, as indicated by the QA Plan Checklist in Section VIII of the Task Technical and Quality Assurance Plan. A surveillance of the Phase II activities was performed by SRNL QA to verify conformance to the QA Plan Checklist. All items that were checked "Yes" in this list were followed with the exception of procedures related to stop work, non-conformance, and the corrective action system. These were not necessary during the performance of Phase II activities since no issues were identified.

Although high level waste samples are being analyzed in this task, the work is not considered waste form affecting and, therefore, does not require the implementation of DOE/RW-0333P requirements. SRNL, however, chose to implement the additional notebook, planning, sample identification, and data review/test validation portions of the RW-0333P requirements to the Phase II activities as best practice. SRNL was also requested to perform work in accordance with the requirements established in the Quality Assurance Project Plan for Testing Programs Generating Environmental Regulatory Data (PL-24590-QA00001)[13] since the activity supports regulatory and environmental testing for the RPP-WTP. This was done for the ICP-AES/ICP-MS portion of the task since it is an established method; however, the laser ablation sample introduction technique is being developed as part of this task and relied on scoping tests to develop the method.

During the performance of the Phase II tasks, routine analytical QA procedures and practices were followed, as applicable. This included using glass standards approved by the customer for the testing, estimating precision and accuracy through extensive studies into deviations between samplings, and following the program plan outline for testing the laser ablation unit approved by the customer. Concurrence/approval was obtained from WTP on the key hold/decision points identified in the Task Plan before proceeding with the next step in the program plan, as well as the exception to the Task Plan before proceeding with the ICP-MS work.

10.0 RECOMMENDATIONS

After working with several different laser ablation units, ICP-AES instruments and ICP-MS instruments, the following recommendations are made:

- The laser ablation unit must have suitable, stable power. For newer LA systems, this is not a problem. WTP should design the laser path of the ablation unit in a manner to ensure that the threshold for ablation to occur is met.
- Sample cell design must take into consideration the amount of samples being analyzed. For this work, each sample had to be individually loaded into the chamber, which took extra time. It has also been suggested that because the system must be purged every time the chamber is open, this may cause a slight change in the background signal.
- For the ICP-MS activities, ensure that the ICP-MS that is used is a scanning instrument and can be used to scan a wide mass range. Although the GV ICP-MS used in this work had excellent sensitivity, it had not yet been set up as a scanning instrument. Analyzing individual elements took a very long time so that only a few elements could be analyzed.
- Ensure that several areas over the sample surface are ablated during analysis. This will aid in determining if there is a sample inhomogeneity issue, as well as aiding in the analysis of a representation of the sample.
- Schedule a minimum of 6 months for testing daily, long term stability of LA, ICP and sample preparation methodologies in WTP Laboratory.
- Continue exploring the use of a set of standards for concentration calculations. Further investigation into what elements tend to work out well in the calibration scenario versus which ones need an internal standard with which to reference should be performed.

11.0 CONCLUSION

The use of laser ablation ICP spectroscopy for analysis of Hanford sludge transformed into glass pellets can and will be very beneficial in determining the sludge composition for production criteria. The data generated in Phase II showed the success of ablation of radioactive samples in an atypical setting. Although, SRNL configuration and set-up was very different, still the report contains valuable information to WTP. The analytical data will provide sequence for sample ablation and ICP measurement during method adaptation in the mock-up facility (222-S) and WTP Analytical Laboratory. Since ICP-MS results were obtained in this Phase II work, comparison with Phase I ICP-AES was not possible. Instead, all recent data taken on radioactive AY-102 samples was obtained and compared as best it could be to the LA data taken from Phase II. Although some of the data comparisons show high deviations and percent differences, explanations exist for the inaccuracy on most of these values. The GV LA ICP-MS method showed good agreement with previous dissolved hot AY-102 glass by the PQ2 ICP-MS and JY ICP-AES methods for several components including Ba, Cr, Sb, Zn and the actinide species in the mass range of mass 233 – 238, as well as the mass range 239 – 241.

Phase II data has shown the applicability of LA-ICP-MS to the Hanford Tank waste matrix for analysis of radioactive samples and the feasibility of performing laser ablation ICP-AES work for the analysis of HLW.

12.0 REFERENCES

1. Herman, C.C., Coleman, C.J., and Zeigler, K.E., “Task Technical and Quality Assurance Plan for Conventional Wet Chemistry and Laser Ablation ICP-AES Development,” WSRC-TR-2004-00447, SRNL-RPP-2004-00073, Revision 0, October 2004.
2. WSRC-SRNL NTP “Wet Chemistry and Laser Ablation Testing,” CCN091850, August 2004.
3. WSRC-SRNL “Test Exception Plan for ICP-MS Analysis,” CCN130232, November 2005.
4. Coleman, C. J., Hay, M. S., and Martin K. B. (2003), “Compositing and Characterization of Samples From Hanford Tank 241-AY-102/C-106”, WSRC-TR-2003-00205 Rev. 0 & SRT-RPP-2003-00086, Rev. 0, October, 2003.
5. Zeigler, K.E., Click, D.J., and Coleman, C.J., “The Development of Laser-Ablation Inductively Coupled Plasma-Atomic Emission Spectroscopy for the Analysis of Hanford High Level Waste: Phase I (U)”, WSRC-TR-2005-00260 Rev. 0 & SRNL-RPP-2005-00038 Rev. 0, August 2005.
6. Edwards, T.B., and Peeler, D.K., "Candidates for RPP Glass Standards," SRNL-SCS-2005-00019, Revision 0, May, 2005.
7. Edwards, T.B., Peeler, D.K., and Best, D. R., "Measured Compositions of Candidates for WTP Glass Standards (U)," SRNL-SCS-2005-00052, Revision 0, October, 2005.
8. Crawford, C., Hansen, E., Schumacher, R., and Bibler, N., “Vitrification and Product Testing of AY-102/C-106 HLW (Env. D) (U),” WSRC-TR-2005-00410, SRNL-RPP-2005-00047, Revision 0, November 2005.
9. Mellinger, G. B. and J. L. Daniel (1983), “Approved Reference and Testing Materials for Use in Nuclear Waste Management Research and Development Programs”, PNL-4955-1, Pacific Northwest Laboratory, December, 1983.
10. Zeigler, K.E., “Rad LA-ICP”, WSRC-NB-2005-00149 Laboratory Notebook, October 2005.
11. Schumacher, R. F., Crawford, C. L., Ferrara, D. M., Bibler, N. E. (2001), Final Report for Crucible Scale Verification of Pretreated C-106 Sludge Mixed with Secondary Wastes, WSRC-TR-2001-00252, SRT-RPP-2001-00068, Westinghouse Savannah River Company, Aiken, South Carolina, November 2001.
12. G. Friedlander, J. W. Kennedy, E. S. Macias and J. M. Miller, ‘Nuclear and Radiochemistry, 3rd Edition, John Wiley & Sons, New York, 1981.
13. D. Blumenkranz, “Quality Assurance Project for Testing Programs Generating Environmental Regulatory Data”, PL-24590-QA00001, Revision 0, June 2001.

APPENDIX A - ANALYSIS OF ACID-DISSOLVED AY102/C106 GLASS BY ICP-AES AND ICP-MS

The AY102/C106 HLW glass used in the laser ablation study was initially characterized (before Sc addition) by dissolving the glass using peroxide fusion and mixed acid dissolution. Dissolved glasses were analyzed by the JY ICP-AES for both peroxide fusion and acid dissolution. Only the acid-dissolved glass was analyzed by PQ2 ICP-MS. The results of the JY ICP-AES analyses have been presented in Ref. 8. No detailed information was given for the PQ2 ICP-MS analyses in the previous work except for reporting of some trace metals.

Since comparison of the current GV LA-ICP-MS data (using the Sc-traced AY102/C106 glass) with the previous acid-dissolved PQ2 ICP-MS data is performed in this study, the complete acid-dissolved PQ2 ICP-MS data set is presented in this Appendix.

Table A- 1 shows the PQ2 ICP-MS characterization data for a triplicate set of acid dissolved AY102/C106 glasses. Symbol meanings are as follows: (<) less than method detection limit, (-) cannot calculate, and (*) detector saturated. The first column in Table A- 1 shows the mass range was analyzed from 43 to 244. The next columns in Table A- 1 show the various isotopes for each mass number and the relative abundance for each naturally occurring isotope. The individual triplicate concentration values are shown for triplicate Samples 1-3, along with the overall average, standard deviation, and percent relative standard deviation (%RSD) for each mass number. The concentration values are in units of µg per g of dissolved glass, i.e., µg/g.

Figure A- 1 shows a plot of the PQ2 ICP-MS data from Table A- 1 over the entire mass range. Figure A- 1 is presented on a vertical scale from 0 – 6000 ug/g. This figure shows that Fe-54 is the highest magnitude isotope measured. Mass number 55 for Mn and 56 for Fe were over-scaled for the 20X dilution factors used in the PQ2 ICP-MS analyses of the acid-dissolved glasses. Iron and manganese are two of the major sludge elements (along with aluminum) that are present in the AY102/C106 glass.[8] Figure A- 1 also shows the higher mass isotopes for Pb (mass 206, 207 and 208) and Th-232 and U-238. Figure A- 2 plots the PQ2 ICP-MS data on a smaller vertical scale, from 0 to 3000 ug/g, and on a smaller mass scale from mass 40 up to mass 160. Various isotopes for Cr, Ni, Fe, Zn, Sr, Zr, Ag, Ba and La are indicated.

The PQ2 ICP-MS data from Table A- 1 can be used to estimate the amount of each element by dividing the concentration for a given mass number by the relative abundance of that element at the given mass number. The estimates were performed for all of the elements indicated in Figure A- 1 and Figure A- 2. The results are compared to the JY ICP-AES values as shown in Table A- 2 for the acid-dissolved glass. Table A- 2 shows that there is good agreement, i.e., within 10%, between the JY ICP-AES and PQ2 ICP-MS values for the elements Ba, Ni, Pb, Zn, and Zr. The values agreed to within 20% for Cr, Fe, La and U. Bolded elements and values in Table A- 2 show agreement between the methods to within 20%. Comparison of the two methods was not as good for Ag, Ce and Sr.

Table A- 1. PQ2 ICP-MS data for acid dissolved AY102/C106 glass (µg/g)

(<) less than method detection limit, (-) less than detection limit, (*) detector saturated

	Isotope			Relative Abundance				(µg/g)		(µg/g)		(µg/g)	(µg/g)		
Mass	a	b	c	a	b	c		Samp1		Samp2		Samp3	Avg.	StdDev	%RSD
43	Ca			0.14				7.2		6.6		5.8	6.5	0.7	11.0
44	Ca			2.08				89.1		82.7		76.9	82.9	6.1	7.4
45	Sc			100.00				117.1		110.3		90.7	106.1	13.7	12.9
47		Ti			7.30			41.0		41.9		38.4	40.5	1.8	4.5
48	Ca	Ti		0.20	73.70			262.3		275.7		249.3	262.5	13.2	5.0
49		Ti			5.50			223.1		214.1		226.4	221.2	6.3	2.9
50	V	Ti	Cr	0.25	5.30	4.35		77.5		72.8		83.2	77.8	5.2	6.7
51	V			99.70				64.6		62.5		55.9	61.0	4.5	7.4
52			Cr			83.80		1261.4		1227.1		1243.6	1244.0	17.2	1.4
53			Cr			9.50		158.1		143.8		155.5	152.5	7.6	5.0
54	Fe		Cr	5.80		2.36		6596.1		6364.4		6065.6	6342.0	265.9	4.2
55		Mn			100.00			*		*		*	*	*	*
56	Fe			91.70				*		*		*	*	*	*
57	Fe			2.14				2336.9		2242.3		2189.6	2256.3	74.6	3.3
58	Fe		Ni	0.31		67.80		2633.5		2519.1		2458.0	2536.9	89.1	3.5
59		Co			100.00			32.6		30.7		29.2	30.8	1.8	5.7
60			Ni			26.40		826.2		799.9		782.9	803.0	21.8	2.7
61			Ni			1.16		31.9		30.2		30.5	30.9	0.9	2.9
62			Ni			3.71		118.6		109.7		110.8	113.0	4.8	4.3
63	Cu			69.10				953.4		884.5		894.9	911.0	37.1	4.1
64		Zn	Ni		48.90	0.95		2931.2		2736.5		2755.8	2807.8	107.2	3.8
65	Cu			30.90				427.4		407.0		398.5	411.0	14.9	3.6
66		Zn			27.80			1624.7		1572.7		1534.7	1577.4	45.2	2.9
67		Zn			4.10			224.5		219.4		215.9	219.9	4.3	2.0
68		Zn			18.60			1006.5		997.2		955.0	986.2	27.5	2.8
69	Ga			60.00				19.3		17.9		17.1	18.1	1.1	6.2
70		Zn	Ge		0.62	20.70		46.0		43.9		43.1	44.3	1.5	3.4
71	Ga			40.00				10.1		9.8		9.2	9.7	0.5	5.0
72			Ge			27.50		11.3		10.7		9.9	10.6	0.7	6.8
73			Ge			7.70		6.7		5.2		6.0	6.0	0.7	12.3
74		Se	Ge		0.90	36.40		2.8		3.0		2.3	2.7	0.4	14.8
75	As			100.00				20.5		21.9		19.3	20.6	1.3	6.2
76		Se	Ge		9.00	7.70	<	0.9	<	1.0	<	0.9	0.0	-	-
77		Se			7.50			2.3		1.8		3.2	2.4	0.7	30.3
78	Kr	Se		0.35	23.50		<	9.1	<	9.2	<	8.8	0.0	-	-
82	Kr	Se		11.60	9.20		<	8.6	<	8.7	<	8.4	8.6	0.2	2.1
85	Rb			72.20				1.4		2.0		1.8	1.7	0.3	15.4
86	Kr	Sr		17.30	9.86			59.2		57.7		56.9	57.9	1.2	2.0
87	Rb	Sr		27.80	7.00			46.5		44.8		44.0	45.1	1.3	2.8
88	Sr			82.60				584.0		567.5		549.8	567.1	17.1	3.0
89	Y			100.00				132.5		133.3		130.4	132.1	1.5	1.1
90	Zr			51.40				1162.0		1152.0		1118.0	1144.0	23.1	2.0
91	Zr			11.20				432.6		418.7		409.9	420.4	11.4	2.7
92	Zr	Mo		17.20	14.80			584.1		599.0		567.6	583.6	15.7	2.7
93	Nb			100.00				302.2		288.8		279.0	290.0	11.6	4.0
94	Zr	Mo		17.40	9.25			615.8		635.1		630.3	627.1	10.0	1.6
95	Mo			15.90				9.6		9.4		9.3	9.4	0.1	1.5
96	Mo	Ru	Zr	16.70	5.52	2.80		312.3		309.7		298.6	306.9	7.3	2.4
97	Mo			9.55		1.66		1.7		1.3		1.5	1.5	0.2	10.8
98	Mo	Ru		24.10	1.88		<	4.7	<	4.7	<	4.5	4.6	0.1	2.1
99	Ru			12.70			<	5.8	<	5.8	<	5.6	5.7	0.1	2.1
100	Ru	Mo		12.60	9.63		<	7.4	<	7.5	<	7.2	7.4	0.2	2.1
101	Ru			17.00				8.5		9.6		8.9	9.0	0.5	6.1
102	Ru	Pd		31.60	1.02		<	18.5	<	18.6	<	17.9	18.3	0.4	2.1
103	Rh			100.00				10.9		9.9		9.8	10.2	0.6	5.9

Table A- 1. PQ2 ICP-MS data for acid dissolved AY102/C106 glass - continued

(<) less than method detection limit, (-) less than detection limit, (*) detector saturated

	Isotope			Relative Abundance				(μg/g)		(μg/g)		(μg/g)	(μg/g)		
Mass	a	b	c	a	b	c		Samp1		Samp2		Samp3	Avg.	StdDev	%RSD
104	Ru	Pd		18.70	11.10		<	12.0	<	12.1	<	11.6	11.9	0.2	2.1
105	Pd			22.30			<	1.7	<	1.7	<	1.6	1.7	0.0	2.1
106	Pd	Cd		27.30	1.25			13.6		13.7		13.8	13.7	0.1	0.8
107	Ag			51.80				656.8		670.1		650.7	659.2	9.9	1.5
108	Pd	Cd		26.50	0.89			7.7		6.9		7.1	7.2	0.4	5.8
109	Ag			48.20				619.6		618.5		580.6	606.2	22.2	3.7
110	Cd	Pd		12.50	11.70			17.8		17.4		16.7	17.3	0.6	3.4
111	Cd			12.80				13.7		12.6		13.3	13.2	0.5	4.1
112	Cd	Sn		24.10	0.97			28.9		27.9		27.6	28.1	0.7	2.5
113	Cd	In		12.30	4.30			15.2		16.3		18.0	16.5	1.4	8.7
114	Cd	Sn		28.70	0.65			28.6		27.4		27.1	27.7	0.8	3.0
116	Sn	Cd		14.50	7.49			22.3		22.1		21.1	21.8	0.6	2.9
117	Sn			7.68				6.1		6.1		5.9	6.0	0.1	2.2
118	Sn			24.20				16.4		16.0		15.7	16.0	0.3	2.1
119	Sn			8.58				16.2		15.6		15.7	15.8	0.3	2.1
120	Sn	Te		32.60	0.10			22.3		21.1		20.6	21.3	0.9	4.0
121	Sb			57.30				7.4		7.2		6.9	7.2	0.2	3.3
122	Sn	Te		4.63	2.60			5.7		5.6		5.5	5.6	0.1	2.3
123	Sb	Te		42.70	0.91			5.9		5.5		5.2	5.5	0.4	6.5
124	Sn	Te	Xe	5.79	4.82	0.10		8.5		8.4		7.8	8.2	0.4	4.3
125	Te			7.14				2.2		2.3		2.5	2.3	0.1	6.1
126	Te	Xe		19.00	0.09			15.0		14.9		14.3	14.7	0.4	2.8
128	Te	Xe		31.70	1.91			21.1		20.6		20.0	20.5	0.6	2.7
130	Te	Xe	Ba	33.80	4.10	0.11		100.9		99.0		98.4	99.4	1.3	1.3
133	Cs			100.00				10.5		10.6		10.3	10.5	0.2	1.5
134	Xe	Ba		10.40	2.42			24.7		23.5		22.1	23.4	1.3	5.7
135	Ba			6.59				7.1		7.0		7.2	7.1	0.1	1.0
136	Xe	Ba	Ce	8.90	7.85	0.19		6.6		6.4		6.5	6.5	0.1	1.3
137	Ba			11.20				131.8		126.6		129.8	129.4	2.6	2.0
138	Ba	La	Ce	71.70	0.09	0.25		453.4		436.8		435.7	442.0	9.9	2.2
139	La			99.90				522.6		509.0		507.0	512.9	8.5	1.7
140	Ce			88.50				464.8		460.1		445.1	456.7	10.3	2.3
141	Pr			100.00				326.1		323.1		324.6	324.6	1.5	0.5
142	Nd	Ce		27.10	11.10			352.6		345.3		344.3	347.4	4.5	1.3
143	Nd			12.20				315.4		312.4		314.2	314.0	1.5	0.5
144	Nd	Sm		23.80	3.10			310.3		308.1		308.8	309.1	1.1	0.4
145	Nd			8.30				216.3		219.7		216.9	217.6	1.8	0.8
146	Nd			17.20				172.2		183.7		180.3	178.7	5.9	3.3
147	Sm			15.00				123.3		126.2		121.1	123.5	2.6	2.1
148	Sm	Nd		11.30	5.76			99.5		99.8		96.6	98.6	1.8	1.8
149	Sm			13.80				6.4		6.7		6.4	6.5	0.2	2.8
150	Sm	Nd		7.40	5.64			98.6		97.7		97.8	98.0	0.5	0.5
151	Eu			47.80				12.4		12.5		12.7	12.5	0.2	1.2
152	Sm	Gd		26.70	0.20			29.6		29.6		29.4	29.5	0.1	0.5
153	Eu			52.20				11.0		11.0		10.8	10.9	0.1	1.2
154	Sm	Gd		22.70	2.18			6.8		7.2		7.2	7.1	0.3	3.6
155	Gd			14.80				22.8		23.3		22.9	23.0	0.3	1.2
156	Gd	Dy		20.50	0.06			22.0		21.4		22.6	22.0	0.6	2.7
157	Gd			15.70				10.2		9.5		9.9	9.9	0.3	3.3
158	Gd	Dy		24.70	0.10			18.5		19.3		19.6	19.1	0.5	2.8
159	Tb			100.00			<	7.9	<	8.0	<	7.7	7.9	0.2	2.1
160	Gd	Dy		21.90	2.34			8.2		8.4		7.3	8.0	0.6	7.4
161	Dy			18.90				5.9		5.7		5.6	5.7	0.1	2.3
162	Dy	Er		25.50	0.14			4.1		4.1		4.2	4.2	0.1	1.4
163	Dy			24.90			<	2.0	<	2.0	<	1.9	2.0	0.0	2.1
164	Dy	Er		28.20	1.61			2.7		2.2		2.4	2.5	0.2	9.3
165	Ho			100.00			<	6.9	<	7.0	<	6.7	6.9	0.1	2.1

Table A- 1. PQ2 ICP-MS data for acid dissolved AY102/C106 glass - continued

(<) less than method detection limit, (-) less than detection limit, (*) detector saturated

	Isotope			Relative Abundance				(μg/g)		(μg/g)		(μg/g)	(μg/g)		
Mass	a	b	c	a	b	c		Samp1		Samp2		Samp3	Avg.	StdDev	%RSD
166	Er			33.60			<	2.0	<	2.0	<	1.9	2.0	0.0	2.1
167	Er			23.00			<	1.6	<	1.6	<	1.5	1.6	0.0	2.1
168	Er	Yb		26.80	0.13		<	2.2	<	2.2	<	2.1	2.2	0.0	2.1
169	Tm			100.00			<	6.7	<	6.8	<	6.5	6.7	0.1	2.1
170	Er	Yb		14.90	3.05		<	1.4	<	1.4	<	1.3	1.4	0.0	2.1
171	Yb			14.30			<	1.2	<	1.2	<	1.2	1.2	0.0	2.1
172	Yb			21.90			<	1.4	<	1.4	<	1.3	1.4	0.0	2.1
173	Yb			16.10			<	1.2	<	1.2	<	1.2	1.2	0.0	2.1
174	Yb	Hf		31.80	0.16		<	2.3	<	2.3	<	2.2	2.3	0.0	2.1
175	Lu			97.40			<	6.4	<	6.5	<	6.3	6.4	0.1	2.1
176	Yb	Hf	Lu	12.70	5.21	2.59	<	1.7	<	1.7	<	1.6	1.7	0.0	2.1
177	Hf			18.60			<	1.8	<	1.8	<	1.7	1.8	0.0	2.1
178	Hf			27.30			<	2.3	<	2.3	<	2.2	2.3	0.0	2.1
179	Hf			13.60			<	0.9	<	0.9	<	0.9	0.9	0.0	2.1
180	Hf	W	Ta	35.10	0.13	0.01	<	2.9	<	2.9	<	2.8	2.9	0.1	2.1
181	Ta			99.90				94.3		68.5		52.2	71.7	21.2	29.6
182	W			26.30				73.8		71.4		72.1	72.4	1.3	1.7
183	W			14.30				40.0		39.8		39.4	39.7	0.3	0.7
184	W	Os		30.70	0.02			84.7		81.8		81.5	82.7	1.8	2.1
185	Re			37.40			<	2.3	<	2.3	<	2.2	2.3	0.0	2.1
186	W	Os		28.60	1.58			77.8		78.4		76.7	77.6	0.9	1.1
187	Re	Os		62.60	1.60		<	6.6	<	6.7	<	6.4	6.6	0.1	2.1
191	Ir			37.30			<	3.1	<	3.1	<	3.0	3.1	0.1	2.1
193	Ir			62.70			<	5.1	<	5.1	<	4.9	5.0	0.1	2.1
194	Pt			32.90				26.7		14.8		18.2	19.9	6.1	30.7
195	Pt			33.80				26.6		15.2		19.0	20.3	5.8	28.6
196	Pt	Hg		25.30	0.14			19.5		10.9		13.2	14.6	4.4	30.5
198	Hg	Pt		10.00	7.20			14.0		8.0		9.9	10.6	3.1	28.8
203	Tl			29.50			<	3.0	<	3.0	<	2.9	3.0	0.1	2.1
204	Hg	Pb		6.85	1.40			387.1		386.5		365.1	379.6	12.5	3.3
205	Tl			70.50			<	6.6	<	6.7	<	6.4	6.6	0.1	2.1
206	Pb			24.10				996.8		1010.0		960.2	989.0	25.8	2.6
207	Pb			22.10				1024.0		1028.0		1018.0	1023.3	5.0	0.5
208	Pb			52.40				2471.0		2410.0		2292.0	2391.0	91.0	3.8
230							<	0.2	<	0.2	<	0.2	0.2	0.0	2.1
232	Th			100.00				619.3		659.8		629.1	636.1	21.1	3.3
233								0.3		0.4		0.3	0.3	0.1	21.8
234	U			0.01				0.1		0.1		0.1	0.1	0.0	2.1
235	U			0.72				11.5		11.7		11.7	11.6	0.1	1.0
236								0.5		0.5		0.5	0.5	0.0	5.5
237								7.3		7.2		7.1	7.2	0.1	1.5
238	U			99.30				1683.0		1708.0		1627.0	1672.7	41.5	2.5
239								30.9		31.5		30.1	30.8	0.7	2.3
240								2.1		2.1		2.1	2.1	0.0	0.9
241								1.4		1.4		1.4	1.4	0.0	2.0
242							<	0.2	<	0.2	<	0.2	0.2	0.0	2.1
243							<	0.2	<	0.2	<	0.2	0.2	0.0	2.1
244							<	0.2	<	0.2	<	0.2	0.2	0.0	2.1

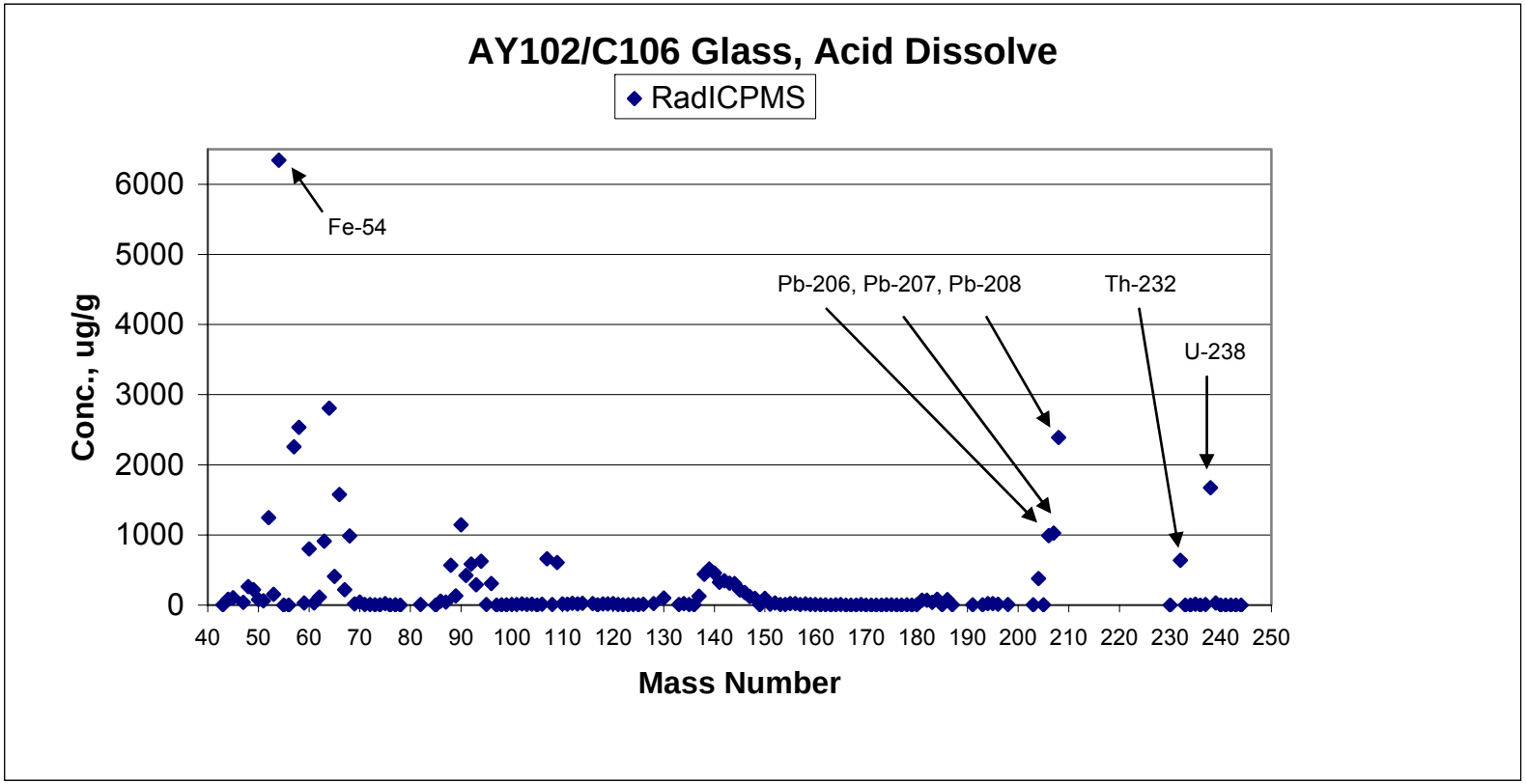

Figure A- 1. PQ2 ICP-MS acid dissolved AY-102/C106 glass data over entire mass range with various elements identified

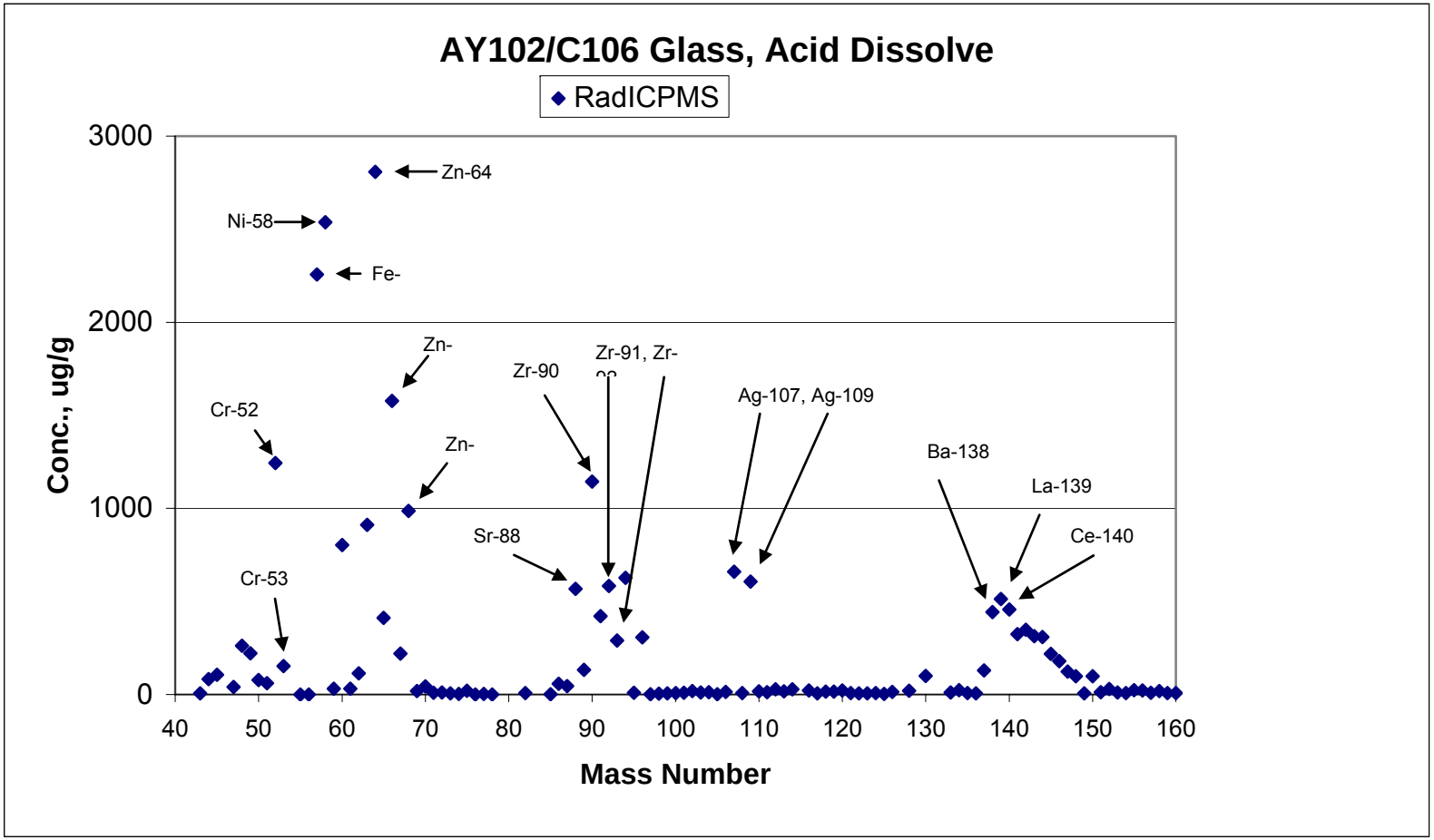

Figure A- 2. PQ2 ICP-MS acid dissolved AY-102 glass data for mass range 40-160

.

Table A- 2. Comparison of glass dissolution data from the JY ICP-AES and PQ2 ICP-MS

	ICP-AES Acid				ICP-MS Acid			% diff
Element	Average	Std Dev	% RSD		Average	Std Dev	% RSD	
	(ug/g)	(ug/g)			(ug/g)	(ug/g)		
Ag	**729**	18	2		**1265**	10	1	-42
Al	27533	231	1					
Ba	**631**	9	1		**616**	14	2	2
Be	1	0	11					
Ca	3310	46	1					
Cd	114	4	3					
Ce	**1320**	46	3		**516**	12	2	156
Cr	**1373**	50	4		**1545**	85	6	-11
Cu	1343	21	2					
Fe	**92700**	1136	1		**107390**	2766	3	-14
Gd	73	1	1					
K	844	17	2					
La	**612**	7	1		**513**	8	2	19
Li	12367	153	1					
Mg	918	13	1					
Mn	19300	300	2					
Mo	524	26	5					
Na	86200	1353	2					
Ni	**3273**	71	2		**3392**	495	13	-3
P	1870	56	3					
Pb	**4610**	236	5		**4432**	287	6	4
S	230	13	6					
Sb	645	17	3					
Si	203000	1732	1					
Sn	10633	379	4					
Sr	**1283**	15	1		**687**	21	3	87
Ti	255	7	3					
U	**2140**	87	4		**1760**	192	11	22
V	22	0	2					
Zn	**5580**	66	1		**5573**	192	3	0
Zr	**2913**	40	1		**3124**	799	21	-7

Percent difference between ICP-AES and –MS is reported in the last column for elements analyzed on both instruments. Bolded elements and values show agreement between the methods to within 20%.